DNA transfection to mesenchymal stem cells using a novel type of pseudodendrimer based on *bis*-MPA

Alexandre Lancelot[1‡], Rebeca González-Pastor[2‡], Alberto Concellón[3], Teresa Sierra[3], Pilar Martín-Duque[4], José L. Serrano[1*]*

1 - Instituto de Nanociencia de Aragón, Universidad de Zaragoza, Spain

2 - Centro de Investigación Biomédica de Aragón, IIS Aragón, Spain

3 - Instituto de Ciencia de Materiales de Aragón, Facultad de Ciencias, Universidad de Zaragoza-CSIC, Spain

4 - Centro de Investigación Biomédica de Aragón, IIS Aragón, Fundación Araid, Universidad Francisco de Vitoria, Spain

KEYWORDS. pDNA transfection, mesenchymal cells, dendronized hyperbranched polymers, *bis*-MPA polyesters, pseudodendrimers.

ABSTRACT. In the search for effective vehicles to carry genetic material into cells, we present here new pseudodendrimers that consist of a hyperbranched polyester core surrounded by amino-

terminated *bis*-MPA dendrons. The pseudodendrimers are readily synthesized from commercial hyperbranched *bis*-MPA polyesters of the 2nd, 3rd and 4th generations and 3rd generation *bis*-MPA dendrons, bearing 8 peripheral glycine moieties, coupled by the Copper(I) -catalyzed Azide-Alkyne Cycloaddition (CuAAC) . This approach provides globular macromolecular structures bearing 128, 256 and 512 terminal amino groups and these can complex pDNA. The toxicity of the three pseudodendrimers was studied on two cell lines, mesenchymal stem cells and HeLa, and it was demonstrated that these compounds do not affect negatively cell viability up to 72 h. The complexation with DNA was investigated in terms of N/P ratio and dendriplex stability. The three generations were found to promote internalizing of pDNA into mesenchymal stem cells (MSCs) , and their transfection capacity was compared with two non-viral commercial transfection agents, Lipofectamine and TransIT-X2. The highest generations were able to transfect these cells at levels comparable to both commercial reagents.

1. INTRODUCTION

Gene therapy is one of the most promising tools in biomedicine, whereby a wide variety of diseases may be treated or prevented using nucleic acids in order to express a therapeutic protein or to silence a defective gene.[1] However, in the last few decades the efficacy of gene therapy alone has been limited, mostly due to inefficient targeting of the desired pathological area. Indeed, this is the main reason why other systems have been used in combined treatments such as, for example, mesenchymal stem cells (MSCs),[2-3] which have been used in numerous clinical trials.

A vector is required to deliver the genetic material into the cells and these vectors can be viral or synthetic.[4] The ideal vector should have high transfection efficiency, low toxicity, minimal effects on normal physiology, be reproducible and easy to use and also have the capability to

expand. Despite the advances in this field, the delivery of nucleic acids to cells remains a challenge.[5-6] On the one hand, viral vectors represent efficient transfection vehicles but they do suffer from some drawbacks, principally in terms of safety.[7] On the other hand, non-viral vectors show a lower efficiency but they have the advantages of a lower immunogenicity risk, an easier scale-up for manufacturing and they are less affected by size-limitations of the genetic material to be delivered.[8] Non-viral vectors include a wide variety of products such as polymers, dendrimers and pseudodendrimers, cationic lipids, polypeptides and nanoparticles.[9] In almost all cases the binding of DNA or RNA with the vector is led by electrostatic interactions between the negatively charged phosphate groups of the nucleic acid and the cations of the vectors. This results in the formation of nanoobjects, called complexes, in which the vector protects the DNA or RNA and facilitates its delivery inside the cells and its expression.[10]

In this field, the special properties of dendrimers,[11,12] such as monodispersity, hypervalency, controlled structure, shape and size, amongst others, make them applicable to promote gene transfection.[13-15] The first dendrimer to be used in gene transfection was polyamidoamine (PAMAM) when, in 1993, Haensler and Szoka expressed exogenous genes into a wide range of cells.[16] Other dendrimers based on polypropyleneimine (PPI),[17] poly-L-lysine (PLL),[18] carbosilane,[19] triazine[20] or phosphorus-containing dendrimers[21] and guanidine layered dendrimers[22] have been used, among others, as non-viral gene therapy vectors. Unfortunately, the cytotoxicity of many of these dendrimers is very high and this precludes their use in gene delivery, although significant efforts have been made to minimize this problem.[8, 23-24]

Bis-MPA [2,2-bis(hydroxymethyl)propionic acid] based polyester dendrimers are widely used in biomedicine and they may be good candidates for gene delivery.[25-27] Indeed, these compounds have high solubility in biological media, *in vitro* and *in vivo* biocompatibility and they are

biodegradable.[28] However, in spite of these interesting properties, the efficiency of amino-functionalized *bis*-MPA dendrimers in gene delivery has hardly been studied and the examples showed poor DNA transfection capacity.[29-31] In fact, very few successful approaches to DNA transfection have been reported and these concern high molecular weight linear polyester derivatives laterally functionalized with amine groups.[32-34]

Taking these precedents into account, we designed a series of three new high generation dendritic derivatives based on commercial *bis*-MPA hyperbranched polyesters and *bis*-MPA dendrons. In contrast with classical dendrimers, hyperbranched polymers are synthesized in only one step. These materials are more polydisperse than dendrimers but they still have a globular shape and numerous peripheral groups.[35] As well as *bis*-MPA dendrimers, *bis*-MPA hyperbranched polyesters are biocompatible and biodegradable and they have proven benefits when used in biomedicine.[27, 29, 36-37] Hyperbranched polymers can be decorated at their periphery with dendrons in order to obtain dendronized hyperbranched polymers, which are also called pseudodendrimers. These hybrid materials are a good compromise between high generation dendrimers and hyperbranched polymers. Due to the hyperbranched core, the synthesis of these compounds is quite easy and fast while the polydispersity remains low and the size and shape of the molecules can be controlled due to the presence of peripheral dendrons.[38-40]

We describe here three new *bis*-MPA-based globular pseudodendrimers for the transfection of pDNA into mesenchymal cells. The pseudodendrimers contain three distinct hyperbranched *bis*-MPA nuclei of the 2nd, 3rd and 4th generation, which were externally functionalized by means of a 'click' reaction with *bis*-MPA dendrons of the 3rd generation bearing 8 peripheral glycine moieties (Scheme 1). These materials could theoretically bear 128, 256 and 512 terminal amino groups, depending on the generation of the central hyperbranched polyester. The three high

generation *bis*-MPA pseudodendrimers have numerous terminal amino groups and they are able to complex and transfect pDNA into the cells. As these materials are based on biodegradable and biocompatible derivatives, they do not exhibit cytotoxicity and as they are based on low dispersity dendritic materials, they afford tunable and reproducible transfection properties.

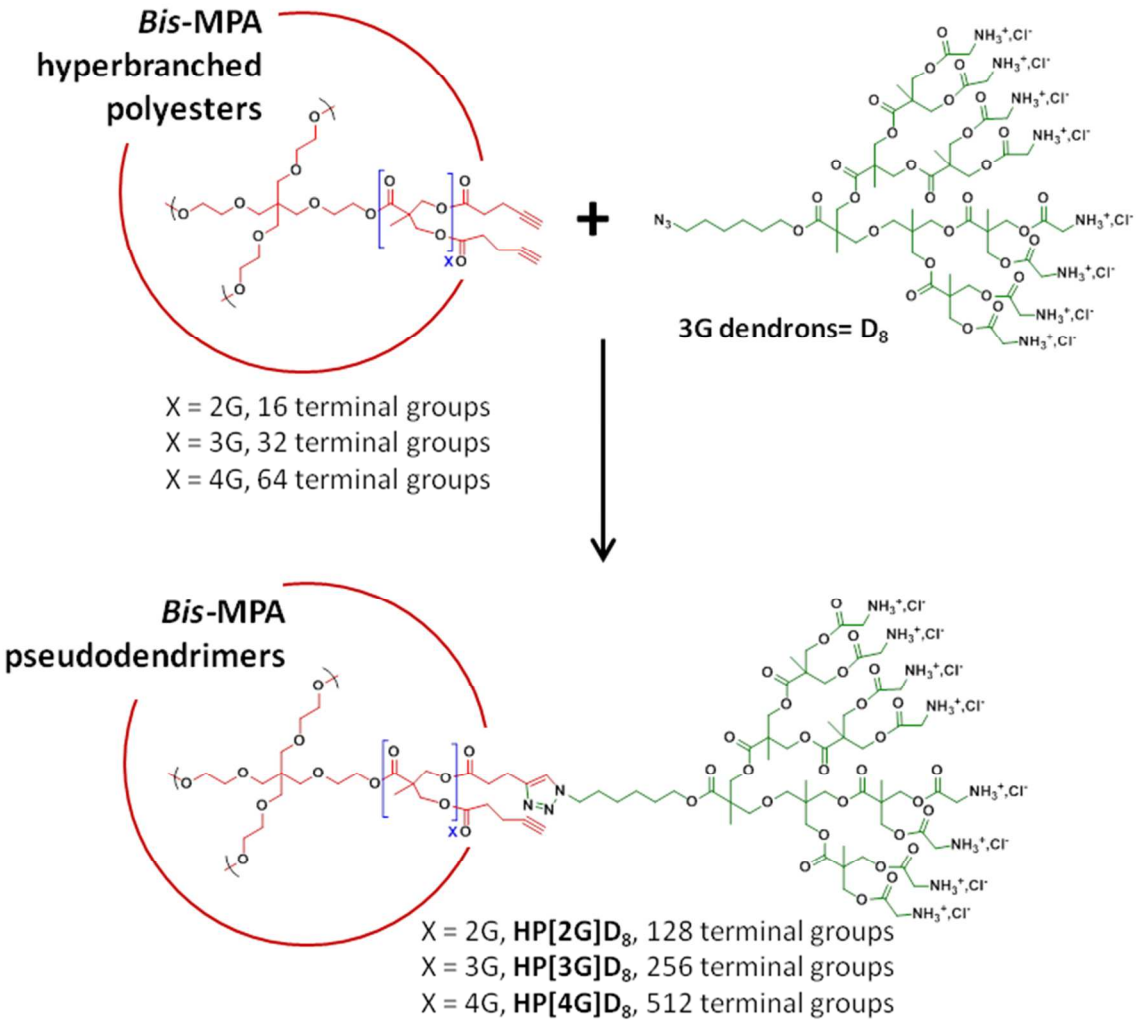

Scheme 1. Representation of the parent components of the *bis*-MPA pseudodendrimers: the hyperbranched polyesters with alkyne terminal groups, the 3rd generation *bis*-MPA dendrons bearing eight glycine moieties and the resulting *bis*-MPA pseudodendrimers that theoretically bear 128, 256 and 512 glycine moieties. Simplified nomenclature: HP[2G]D_8, HP[3G]D_8 and HP[4G]D_8.

Tracking experiments were carried out using two pseudodendrimers of the 2nd and 3rd generation labeled with rhodamine B, *i.e.*, HP[2G]D_8-RhB and HP[2G]D_8-RhB, in combination with a labeled pDNA. The results showed a fast energy-dependent uptake and accumulation of both pseudodendrimers and dendriplexes, and highlighted the importance of the negative charge of the cell membrane for efficient internalization. To our knowledge, this is the first time that dendrimeric *bis*-MPA polyester derivatives have been used successfully in pDNA transfection, at least for bone marrow-derived mesenchymal stem cells.

2. EXPERIMENTAL SECTION

2.1. Materials. Unless otherwise stated, the reagents used for the synthesis of the pseudodendrimers were purchased from Sigma-Aldrich® or Acros Organics™ and were used without further purification. The hyperbranched polyesters derived from 2,2-bis(hydroxymethyl)propionic acid, G = 2, 3 and 4, with average molecular weights of 1750, 3610, 7325 $g.mol^{-1}$ and 16, 32, 64 average terminal groups, respectively, were purchased from Sigma-Aldrich®. Solvents were purchased from Scharlab, S.L.; dichloromethane was distilled prior to use as a reaction solvent. Enhanced green fluorescent protein DNA plasmid (pEGFP-N1 4733bp) was obtained from BD Biosciences Clontech®.

2.2. Synthesis. In this section only the general procedures employed for the synthesis of the pseudodendrimers starting from the commercial hyperbranched polymers are described. The synthesis of the azido-functionalized dendron (D_8Boc), general procedures (I), (II) and (III)[41] as well as the exhaustive synthetic protocols for the pseudodendrimers with and without rhodamine B are fully described in the supporting information (SI-1 and SI-2). General procedures (IV), (V), (VI) and (VII) are described below and the characterization data for one derivative are

included as an example. Complete characterization data for all the derivatives are gathered in the supporting information (SI-2).

General procedure (IV) for the functionalization of the commercial hyperbranched polyesters with terminal alkyne groups (See Scheme 2):[42] HP[2G]-$(OH)_{16}$, HP[3G]-$(OH)_{32}$ and HP[2G]-$(OH)_{64}$ (1.00 eq.), DPTS (0.50 eq. per hydroxyl group) and 4-pentynoic acid (1.25 eq. per hydroxyl group) were dissolved in dry THF (100 mL). The reaction mixture was stirred at 0 ºC under an argon atmosphere. EDC·HCl (1.25 eq. per hydroxyl group) was added. The mixture was stirred at room temperature for 72 h under an argon atmosphere. The solvent was evaporated. The crude product was redissolved in dichloromethane and purified by various washings with aqueous solutions and by precipitation into cold hexane. HP[2G]-≡, HP[3G]-≡ and HP[4G]-≡ were obtained as brown sticky solids.

HP[3G]-≡ ^{1}H NMR ($CDCl_3$, 400 MHz, see Scheme 2 for ^{1}H numbering) δ (ppm): 1.24 (m, 84H, H-7), 1.99 (m, 31H, H-13'), 2.44 (m, 64H, H-11'), 2.54 (m, 64H, H-10'), 3.64 (m, 16H, H-2 and H-3), 4.24 (m, 126H, H-4 and H-8). ^{13}C NMR ($CDCl_3$, 100 MHz) δ (ppm): 14.4, 17.9, 33.3, 46.7, 65.5, 69.5, 82.5, 171.3. FTIR (ν_{max}/cm^{-1}, KBr): 3285 (≡C−H st), 2119 (C≡C st), 1740 (C=O st), 1243 (CO–O st) SEC (*ref PMMA*): M_w 7700 g mol^{-1}; $Đ_M$ 1.43.

General procedure (V) for grafting of the D_8Boc dendrons onto the hyperbranched polyester cores by the CuAAC reaction (see Scheme 2): HP[2G]-≡, HP[3G]-≡ *and* HP[4G]-≡ (1.00 eq.) were dissolved in DMF (30 mL). D_8Boc (1.20 eq. per alkyne group) was added to the solution. Three vacuum-argon cycles were carried out to remove the O_2. The reaction mixture was stirred at 45 ºC. $CuSO_4.5H_2O$ (0.10 eq. per alkyne groups) was dissolved in DMF (10 mL). L-Ascorbate (0.20 eq. per alkyne group) and TBTA (0.10 eq. per alkyne group) were added to the copper solution. Three vacuum-argon cycles were carried out in order to remove the O_2 and the copper

solution was stirred at 45 ºC until it became yellow. The solution was then added by cannula to the previous azide-alkyne reaction mixture. The reaction mixture was stirred at 45 ºC for 2 d. The crude products were extracted with ethyl acetate and then purified by various washings with aqueous solutions, including KCN solution, filtration through silica gel and precipitation into a mixture of hexane and ethyl acetate (9:1). HP[2G]-*D_8Boc,* HP[3G]-*D_8Boc and* HP[4G]-*D_8Boc* were obtained as white solids.

HP[3G]D_8Boc. ^{1}H NMR (400 MHz, $CDCl_3$, see Scheme 2 for ^{1}H numbering) δ (ppm): 1.24 (m, 859H, H-7, H-16, H-17 and H-22), 1.43 (s, 2232H, H-28), 1.65 (m, 62H, H-18), 1.89 (m, 62H, H-15), 2.73 (m, 62H, H-10) 2.86 (m, 62H, H-11), 3.64 (m, 16H, H-2 and H-3), 3.87 (m, 496H, H-25), 4.26 (m, 1050H, H-4, H-8, H-19 and H-23), 4.44 (m, 62H, H-14), 5.48 (bs, ~NH), 7.42 (s, 31H, H-13). ^{13}C NMR (75 MHz, $CDCl_3$) δ (ppm): 17.5, 17.8, 20.8, 25.3, 26.2, 28.3, 30.2, 33.3, 42.2, 46.4, 46.7, 50.0, 65.4, 65.6, 79.8, 121.2, 145.8, 155.9, 170.1, 171.5, 171.8, 172.0. FTIR (ν_{max}/cm^{-1}, ATR): 3354 (N–H st), 2986 and 2947 (C–H st), 1736 (C=O ester st), 1711 (C=O st carbamate), 1518 (N–H δ), 1462 (CH_2, CH_3 δ), 1367 (C–N st), 1244 (CO–O st), 1155 (N–CO–O st), 1124 (O–C–C st). EA: (%) Found: C, 53.2; H, 7.35; N, 6.5. Calc. for $C_{3317}H_{5247}N_{341}O_{1550}$: C, 53.3; H, 7.1; N, 6.4. SEC (*ref PMMA*): Mw 42745 g.mol^{-1}; $Đ_M$ 1.14.

General procedure for the deprotection of the amines at the periphery (VI) (see Scheme 2): Terminal amines were deprotected by dissolving HP[2G]D_8Boc, HP[3G]D_8Boc, HP[4G]D_8Boc, (1.00 eq.) in ethyl acetate (5 mL). A solution of 3M HCl in ethyl acetate (25 mL) was added. The reaction mixture was stirred at room temperature for 1.5 h. The formation of a white precipitate was observed. HCl was removed from the reaction mixture by stirring under vacuum. The white precipitate was recovered by centrifugation and washed once with pure ethyl acetate. HP[2G]D_8, HP[3G]D_8 *and* HP[4G]D_8 were obtained as white solids.

HP[3G]D_8. ^{1}H NMR (400 MHz, CD_3OD, see Scheme 2 for ^{1}H numbering) δ (ppm): 1.35 (m, 735H, H-7 and H-22), 1.43 (m, 124H, H-16 and H-17), 1.71 (m, 62H, H-18), 1.93 (m, 62H, H-15), 2.77 (m, 62H, H-10), 3.00 (m, 62H, H-11), 3.68 (m, 16H, H-2 and H-3), 3.99 (m, 496H, H-25), 4.17 (m, 62H, H-19), 4.35 (m, 492H, H-4, H-8 and H-23[1,2G]), 4.46 (m, 558H, H-14 and H-23[3G]), 7.94 (s, 31H, H-13). ^{13}C NMR (75 MHz, C_2D_6SO) δ (ppm): 17.1–17.4, 21.2, 24.8, 25.6, 27.9, 30.0, 32.8, 45.9, 46.2, 49.3, 65.7, 122.1, 144.7, 167.0, 171.4, 172.1. FTIR (ν_{max}/cm^{-1}, ATR): 3414 ($N–H^+$ st), 3001 and 2851 (C–H st), 1734 (C=O st ester), 1605 and 1510 ($N–H^+$ st), 1474 (CH_2, CH_3 δ), 1302 (C–N st), 1223 (CO–O st), 1126 (O–C–C st). EA: (%) Found: C, 41.5; H, 7.0; N, 7.6.Calc. for $C_{2077}H_{3507}N_{341}O_{1054}$: C, 42.3; H, 6.0; N, 8.1.

General procedure (VII) for the grafting of D_8Boc dendrons and rhodamine B onto the hyperbranched polyester cores using CuAAC:

HP[2G]-≡ and HP[3G]-≡ (1.00 eq.) were grafted first with D_8Boc (respectively 0.93 and 0.77 eq. per alkyne group) and secondly with N_3-RhB (respectively 3.00 and 1.71 eq. per free alkyne group, prepared as described previously[43]) following the conditions explained in general procedure (V). The intermediates were purified as described in general procedure (V). The final crude products were extracted with ethyl acetate and then purified by various washings with aqueous solutions, including a KCN solution, and dialysis against methanol for 2 days. The pure products HP[2G]D_8Boc-RhB and D[3G]D_8Boc-RhB were obtained as dark pink solids.

HP[3G]D_8Boc-RhB. ^{1}H NMR (400 MHz, $CDCl_3$, see Scheme SI-6 for ^{1}H numbering) δ (ppm): 1.24 (m, 796H, H-7, H-16, H-17, H-22 and H-44), 1.42 (s, 1728H, H-28), 1.65 (m, 62H, H-18), 2.00 (m, 62H, H-15), 2.89 (m, 62H, H-10), 3.17 (m, 62H, H-11), 3.64 (m, 72H, H-2, H-3 and H-43), 3.87 (m, 384H, H-25), 4.25 (m, 854H, H-4, H-8, H-19 and H-23), 4.55 (m, 62H, H-14), 5.50 (bs, ~NH), [6.7–7.2] (bs, H_{ar} RhB), [7.30–8.29] (m, bs, H-13 and m H_{ar} RhB). FTIR

(ν_{max}/cm^{-1}, ATR): 3383 (N–H st), 2978 and 2933 (C–H st), 1740 (C=O st ester), 1713 (C=O st carbamate), 1512 (N–H δ), 1460 (CH_2, CH_3 δ), 1367 (C–N st), 1248 (CO–O st), 1157 (N–CO–O st), 1130 (O–C–C st).

2.3. Pseudodendrimer characterization. ^{1}H Nuclear magnetic resonance (NMR) and ^{13}C NMR experiments were performed on Bruker AV-400 (^{1}H: 400 MHz, ^{13}C: 100 MHz) or Bruker AMX300 (^{1}H: 300 MHz, ^{13}C: 75 MHz) spectrometers using deuterated chloroform ($CDCl_3$), deuterated methanol (CD_3OD) and deuterated dimethyl sulfoxide [$(CD_3)_2SO$] as solvents. The chemical shifts are given in ppm relative to TMS and the coupling constants are in Hz; the residual solvent peak was used as internal standard. Mass spectrometry (MS) was performed on a Bruker Microflex employing the matrix-assisted laser desorption ionization-time of flight (MALDI-TOF) technique with a nitrogen laser (337 nm) and dithranol as matrix or with an ESI Bruker Esquire 3000 plus spectrometer employing the electrospray technique. Infrared (IR) spectra were obtained on an FT-IR ATI-Mattson Genesis Series II or a JACSO FT/IR-4100 apparatus and recorded between 4000 and 600 cm^{-1}. The measurements were performed in attenuated total reflection (ATR) mode or using a suspension of the sample in nujol on NaCl cells. Size exclusion chromatography (SEC) was performed on a Waters e2695 Alliance system employing two in series Styragel columns HR4 and HR1 (500 and 10^4 pore size) and a Waters 2424 evaporation light scattering detector with a sample concentration of 1.00 mg/mL. The solvent was THF (HPLC grade) with a flow rate of 1.00 mL/min at 35 ºC; poly(methyl methacrylate) (PMMA) was used as the standard for calibration. Elemental Analysis (EA) was performed on a Perkin-Elmer 2400 series II microanalyzer. Copper analysis was carried out by Inductively coupled plasma atomic emission spectroscopy (ICP-AES) performed on a Thermo elemental IRIS intrepid apparatus, with a limit of quantification (LOQ) of 15 ppm.

2.4. Dendriplex formation, dendriplex sizes and ζ potentials, dendriplex stability. Dendriplexes were freshly prepared before use. Briefly, pDNA was added to a series of pseudodendrimer solutions diluted with distilled water (DLS, TEM, titration and gel retardation studies), serum-free medium (SFM) (gel retardation assays, cellular internalization and transfection studies) or complete medium (DMEMc) (degradation studies). The solutions were mixed by vigorous pipetting and incubated for 20 min at room temperature.

Gel retardation assay

In order to maintain the pseudodendrimer:pDNA (w:w) ratios, dendritic material concentrations were adjusted to the amount of pDNA. 15 µL of dendriplexes at different ratios, from 1:1 to 1000:1 (w:w), containing 250 ng of pDNA were mixed with appropriate amounts of 6X loading buffer (Takara, UK) and then electrophoresed on a 0.8% (w/v) agarose gel in 1X TAE (40 mM TRIS/HCl, 1% acetic acid, 1 mM EDTA, pH 7.4) containing SyberSafe for 45 min at 95V. Lipofectamine 2000 and TransIT-X2 were used as controls at recommended ratios (w:w and v:w, respectively). The location of pDNA in the gel was analyzed on a G:Box UV transilluminator (Syngene, UK).

Ethidium bromide exclusion assay

pDNA condensation was measured by displacement of EtBr. 4 µg pDNA were complexed with increasing amounts of pseudodendrimer in a final volume of 200 µL. After 30 min of incubation, 20 µL of a 0.1 mg/mL ethidium bromide solution were added and solutions were mixed by pipetting. Fluorescence was measured at 530/590 (excitation/emission) on a Synergy HT plate reader (BioTek, USA). Results are given as relative fluorescence intensity values, where 100% represents the fluorescence of pDNA alone and 0% represents the fluorescence of non-intercalating EtBr as a blank. The relative fluorescence values were estimated from the

equation Fr (%) = ((Fm − Fd) / (F_0 − Fd)) × 100; where Fr is the relative fluorescence, Fm is the measured fluorescence, Fd is the dye fluorescence in the absence of pDNA and F_0 is the initial fluorescence of the dye-pDNA complex in the absence of dendrimer.

ζ Potential titration

All measurements were performed on a Malvern Zetasizer Nano ZS in a NaCl-HEPES buffer containing 6 mM of HEPES buffer pH 7.4 and 144 mM of NaCl. The dendriplexes were prepared at a concentration of 10 μg/mL of pDNA and with concentrations of pseudodendrimers in the range between 4.5 and 2000 μg/mL. The solutions were mixed by vigorous pipetting and incubated for 30 min at room temperature prior to measurement. Three measurements with a minimum of 10 scans were carried out for each sample.

Dynamic light scattering (DLS)

All measurements were performed on a Brookhaven Instruments Corporation 90 plus particle size analyzer. Samples for DLS measurements were freshly prepared in distilled water at a concentration of 1.00 mg/mL at two pseudodendrimer:pDNA (w:w) ratios (10:1 and 100:1). A series of five measurements was performed for each sample. The results are given as intensity.

Cryogenic transmission electron microscopy (cryoTEM)

Images were recorded on a FEI TECNAI T20 microscope with a beam power of 200 kV using holey carbon film 300 mesh copper grid, quantifoil carbon film 200 mesh copper grid or Lacey 300 mesh copper grid provided by Agar Scientific. Grids were ionized using a plasma cleaner. Samples were freshly prepared at room temperature in distilled water at a concentration of 1.00 mg/mL of pseudodendrimer and the corresponding concentration of pDNA. A droplet (60 μL) of the sample was deposited on the grid. Sample vitrification was automatically processed using a vitrobot (FEI) and performed in liquid ethane. A specific sample holder, Gatan for cold samples,

was used to stock the grids in liquid nitrogen between sample vitrification and observation with the microscope.

Dendriplex Stability

In order to determine the stability of the complexes under different conditions, dendriplexes were prepared as described above in SFM or DMEMc at different ratios from 1:1 to 500:1 (w:w) and then maintained at 37 ºC for different times before running the gel.

2.5. Cell lines and cell culture. MSCs (mouse mesenchymal stem cells, obtained from Lonza) were grown in DMEM/F12 (Biowest) supplemented with 10% FBS (Gibco), 1% Penicillin/Streptomycin/Amphotericin (Biowest) and 2 mM L-glutamine (Biowest) and maintained under hypoxic conditions (3% O_2). Human cervix cancer cell line HeLa (kindly obtained from Cancer Research-UK Cell services) was maintained in DMEM High Glucose (w/Glutamine, Biowest) supplemented with 10% FBS and 1% Pencillin/ Streptomycin/Amphotericin at 37 ºC and 5% CO_2 in a humidified atmosphere. Cells were treated and analyzed as indicated for each experiment.

2.6. Cytotoxicity studies. *Alamar Blue® assay*. Cells were seeded at a density of 5×10^3 cells per well in 96 multiwell culture plates. After 24 h incubation, the culture medium was removed and 100 μL of DMEMc with increasing concentrations of the corresponding pseudodendrimer were added (0.1–1 mg/mL). After 24–72 h the solutions were replaced by 100 μL of fresh DMEM and 10 μL of Alamar Blue® dye solution (Thermo Fisher Scientific). Upon entering the cells, resazurin, the active ingredient of the dye, is reduced to resorufin, which produces very bright red fluorescence. After incubation for 3 h at 37 ºC, fluorescence was read at 530/590 (excitation/emission) on a Synergy HT (BioTek, USA) plate reader. Untreated cells incubated with medium without dendrimer were used as control. Cytotoxicity is expressed as the relative

viability of the cells compared to control cells (considered as 100% viability). Three replicates per concentration were assayed in each of the three independent experiments performed. *Flow cytometry analysis*. DNA cell cycle analysis was measured on propidium iodide (PI)-stained nuclei of 10^6 cells using a FACSArray system (Becton Dickinson). In all experiments the control and cells incubated with pseudodendrimers were harvested by trypsinization, washed twice with PBS, fixed in ice-cold 70% EtOH and maintained at 4 ºC for at least 1 h prior to analysis.

2.7. In vitro transfection. MSCs were seeded at a density of 1×10^4 cells per well in 96-well plates 24 h prior to all experiments. In positive control experiments, plasmid DNA was mixed with Lipofectamine (Thermo Fisher Scientific) at a 3:1 w:w ratio in SFM. After incubation at room temperature for 20 min, 10 μL of the pDNA–lipid complex were added to 40 μL of fresh SFM in each well and incubated for 4 h or 24 h. 50 μL of dendriplexes consisting of 0.1–0.4 μg of pEGFP and the adjusted amount of pseudodendrimer to obtain the desired pseudodendrimer:pEGFP (w:w) ratios (10:1, 50:1, 100:1, 500:1) were prepared in SFM or DMEMc and added to each well in duplicate after 30 min incubation. The medium in the sample wells was changed to DMEMc after 4 h or 24 h and EGFP expression was evaluated by fluorescence microscopy (Olympus IX81 Olympus, Spain) and on a microplate reader (485/20, 528/20) at 24 h and 48 h. Alamar Blue® reagent was used to evaluate the cytotoxicity of the complexes at the end of the experiments. For confirmation by flow cytometry, cells were seeded at a density of 5×10^5 cells per well in 6-well plates and incubated with 750 μL of dendriplexes with 1–4 μg of pEGFP for 24–48 h.

2.8. Uptake and internalization. In order to determine the cellular uptake and intracellular distribution of the pseudodendrimers alone or the dendriplexes, the pseudodendrimers modified with rhodamine or unlabeled pseudodendrimer complexed with Cy5-labeled plasmid were

visualized by confocal laser scanning microscopy and flow cytometry. pEGFP was Cy5-labeled using the Label IT Tracker Intracellular Nucleic Acid Localization Kit (Mirus). Briefly, the DNA plasmid was incubated with Label IT tracker reagent at 37 ºC for 1 h, after which unreacted reagent was removed from the labeled plasmid by EtOH precipitation. Plasmid and Label IT-Cy5 Tracker concentrations were checked on a NanoDrop 2000 spectrophotometer at 260 nm and 650 nm, respectively. The average number of labels per plasmid molecule was estimated to be 40 (14 pmol Cy5/µg pEGFP). *Confocal laser scanning microscopy.* MSCs were seeded at a density of 8 × 10^4 cells per well in 24 multiwell culture plates over sterile glass covers and grown for 24 h, after which the medium was replaced with SFM or DMEMc with pseudodendrimer or dendriplexes at ratios 50:1 and 200:1 (w:w). At different time points, cells were washed with PBS and fixed in paraformaldehyde 4%. To stain actin filaments, cells were first permeabilized in PBS-1% BSA-0.1% saponin and then incubated for 1 h at room temperature with Alexa Fluor 488 phalloidin (Thermo Fisher Scientific) diluted in the permeabilization solution (1:200) in the dark. After washing, the coverslips were mounted and the cell nuclei stained at the same time with a solution of Mowiol-DAPI (1:1000), and the cellular uptake and localization were explored by confocal microscopy using a 60× objective (Olympus FV10-i Oil Type, Olympus, Spain). Green fluorescence was observed under 499/520 nm ($\lambda_{exc}/\lambda_{em}$), red fluorescence was observed under 558/575 nm ($\lambda_{exc}/\lambda_{em}$), DAPI under 359/461 nm ($\lambda_{exc}/\lambda_{em}$) and Cy5 under 645/664 nm ($\lambda_{exc}/\lambda_{em}$). Image treatment and quantification was carried out with FV10i-SW software (Olympus). For early endosome labeling, CellLight® reagents (Life Technologies) were used according to the manufacturer's instructions. Briefly, 30 PPC of GFP-reagent for early endosomes (green fluorescence, 489/510 nm ($\lambda_{exc}/\lambda_{em}$)) was added directly to cells in culture and incubated overnight before adding the complexes. The cells were then prepared for confocal

microscopy as explained above. *Flow Cytometry*. Cellular uptake of dendriplexes was also assayed by flow cytometry in a FACSAria cytometer (BD) and the results were analyzed using FACS Diva software. MSC cells were seeded in duplicate in 6-well plates at a density of 4×10^5 cells per well. After internalization of pseudodendrimers:pEGFP-Cy5 for different times at 37 ºC, cells were washed twice with PBS-Glycine pH 2.6 to remove dendriplexes attached to the cell surface, then twice with PBS, trypsinized, washed twice by pelleting and resuspended in PBS. Cy5 was detected at 649/670 nm. Dead cells were gated according to forward and sideward scatter of untreated cell samples and 10000 events were collected per sample.

2.9. Statistical analysis. Results are reported as mean ± SD and experiments were performed at least in triplicate. Normally distributed data were analyzed by two-sample t-test and one-way ANOVA using Minitab 17 software (State College, PA). $P<0.01$ and $P<0.05$ were considered to be statistically significant.

3. RESULTS AND DISCUSSION

3.1. Synthesis and characterization of the pseudodendrimers HP[2G]D_8Boc, HP[3G]D_8Boc and HP[4G]D_8Boc. The synthesis of the pseudodendrimers starting from the commercially available hyperbranched polyesters (HP[nG]-(OH), n = 2, 3, 4) is represented in Scheme 2.

The three pseudodendrimers were synthesized by a two-step convergent synthesis with hyperbranched polymers as cores.[38, 44] In our case, 3rd generation *bis*-MPA dendrons were grafted onto three different cores based on *bis*-MPA hyperbranched polymers of the 2nd, 3rd and 4th generations by a Cu^I-catalyzed variant of the Huisgen 1,3-dipolar cycloaddition of azide and alkyne groups (CuAAC). This reaction has a high specificity and high reactivity even with large

molecules.[45] Following this approach, pseudodendrimers of high generation and low polydispersity can be synthesized in a few steps. Addition of the generations of the hyperbranched polymers and the dendrons allows pseudodendrimers of virtual 5th, 6th and 7th generations to be synthesized as follows.

The acid moiety of the *bis*-hydroxylmethyl propionic acid (*bis*-MPA) was reacted with 6-azido-1-hexanol to insert a clickable azide function at the focal point of the dendron. The dendron was then synthesized by successive Steglich esterification reactions [in the presence of N,N'-dicyclohexylcarbodiimide (DCC) and 4-(dimethylamino)pyridinium p-toluenesulfonate (DPTS)] to grow the dendrimer up to the 3rd generation. Each esterification step was followed by deprotection of the hydroxyl groups by hydrolysis of the ketal protecting groups under mild conditions (see Scheme SI-1). The 3rd generation *bis*-MPA dendron was then functionalized with eight *tert*-butyloxycarbonylamino glycine moieties at its periphery by Steglich esterification in order to favor the complexation of DNA plasmid (general procedures I, II and III).[41, 46] All of these reactions gave good yields (between 98 and 79%). On the other hand, the three commercially available hyperbranched polyester cores of 2nd, 3rd and 4th generation, with 16, 32 and 64 external groups, respectively, were functionalized with 4-pentynoic acid under Steglich esterification conditions in order to introduce terminal alkyne groups (general procedure IV).[42] The reaction yields were in the range between 64 and 81%.

In the coupling reaction between the hyperbranched polymeric cores and the dendrons, the Cu(I) catalytic species was formed *in situ* by reduction of Cu(II) salts with L-ascorbate.[47] Tris[(1-benzyl-1*H*-1,2,3-triazol-4-yl)methyl]amine (TBTA) was employed to increase the stability of the catalytic species.[48] This catalytic system was removed by extraction with aqueous KCN and filtration through silica gel, whereas unreacted dendrons were easily removed by

washing procedures with a mixture of hexane and ethyl acetate. The pseudodendrimers HP[2G]D_8Boc, HP[3G]D_8Boc *and* HP[4G]D_8Boc were obtained in good yields (between 65 and 77%). All the three compounds were analyzed by ICP-AES and negligible copper traces were found, below 40 ppm (see Table SI-1).

In the final step, the *tert*-butoxy carbamate protecting groups were removed by treatment with HCl in ethyl acetate to obtain the corresponding cationic materials HP[2G]D_8, HP[3G]D_8 *and* HP[4G]D_8 in a fast and convenient way and in quantitative yields. ICP-AES analysis didn't quantified copper traces in the final ammonium derivatives (see Table SI-1).

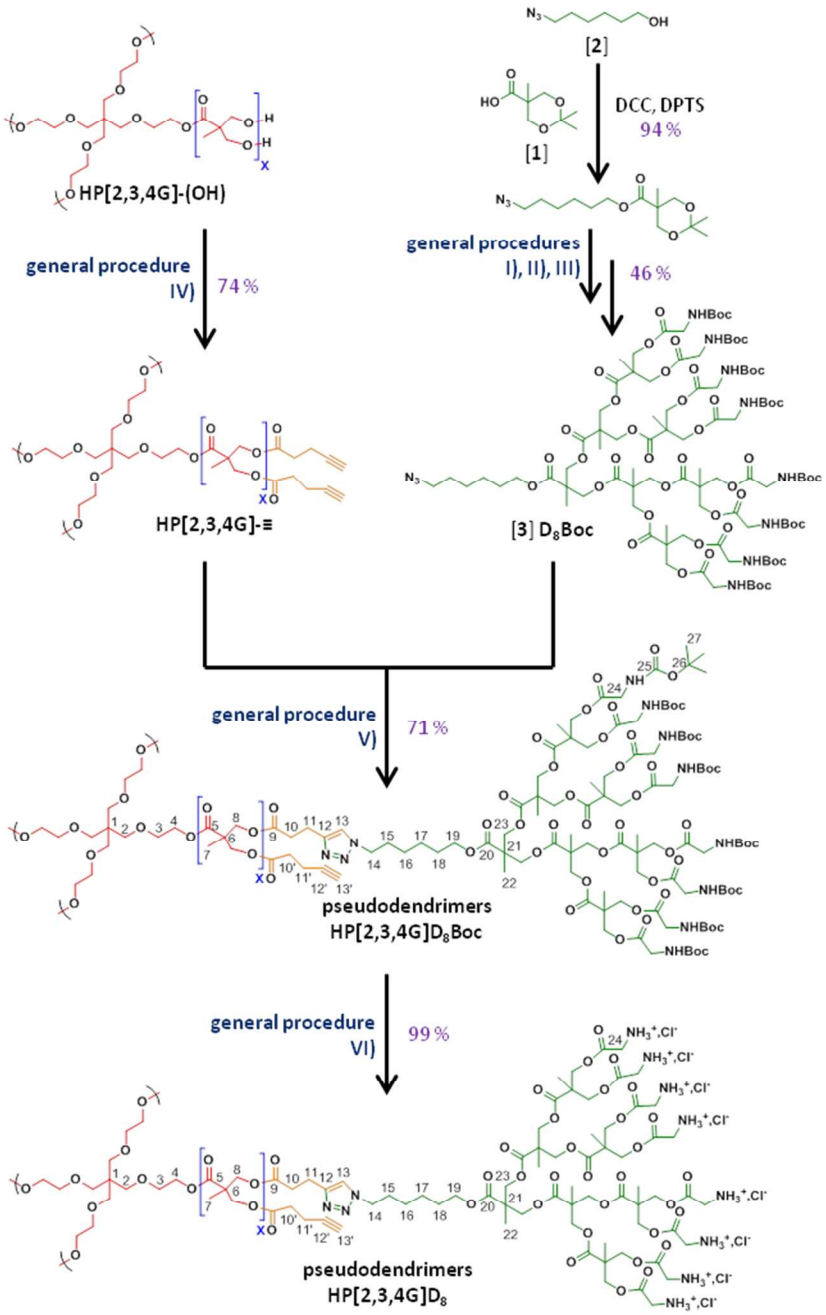

Scheme 2. Synthesis of the *bis*-MPA pseudodendrimers with cores based on the hyperbranched polyesters of the three generations 2G, 3G and 4G grafted with the peripheral dendrons of 3rd generation with glycine moieties. General procedures (I), (II) and (III) are described in the supporting information SI-1.

Functionalization of the commercial hyperbranched polyesters with alkyne groups and subsequent formation of the triazoles that link the dendrons with the hyperbranched polymeric cores were confirmed by NMR spectroscopy. Firstly, the successful addition of the alkyne groups was confirmed by the corresponding signals in the NMR spectra. In comparison with the commercial precursors, three new peaks were observed at 1.99, 2.44 and 2.54 ppm in the ^{1}H NMR spectrum (Figure 1a). These signals correspond to the protons H-13', H-11' and H-10', respectively. Secondly, the presence of a peak at 7.41 ppm in the ^{1}H NMR spectrum (see SI-3, Figure SI-3-1) and two peaks at 145.9 and 121.2 ppm in the ^{13}C NMR spectrum (see SI-3, Figure SI-3-2), which correspond to H-13 (Scheme 2) and C-12 and C-13 (Scheme 2), confirmed the formation of the triazole. Furthermore, the peaks corresponding to the –CH_2– groups in the α- and β-positions of the triazole were shifted to lower field. Thus, protons belonging to the hyperbranched polyester part shifted from 2.44 and 2.54 ppm (protons H-11' and H-10', respectively, in Scheme 2) to 2.73 and 2.96 ppm (protons H-10 and H-11 in Scheme 2) when the triazoles are formed. In a similar way, the protons of the D_8Boc dendrons, the signals of which appeared at 1.66 and 3.12 ppm, respectively, in the free dendron, moved to 1.90 and 4.43 ppm (H-14 and H-15 in the Scheme 2) when the dendron had been grafted onto the hyperbranched polymer (see SI-3, Figure SI-3-1).

^{1}H NMR spectroscopy also allowed the degree of dendron grafting to be estimated (Figure 1A). Functionalization of the commercial hyperbranched polyesters with the peripheral alkyne groups was first assessed by considering the integration of the bis-MPA methyl proton signals (H-7) at 1.24 ppm and the integrations of the two methylene protons (H-10' and H-11') of the 4-pentynoate at 2.55 and 2.44, respectively. High levels of functionalization (> 90%) were obtained in all cases. HP[2G]-≡ was functionalized with 15 terminal alkyne groups compared to

the 16 theoretically possible. HP[3G]-≡ was functionalized with 31 alkyne groups compared to the 32 theoretically possible and HP[4G]-≡ contained 61 alkyne groups compared to the 64 theoretically possible.

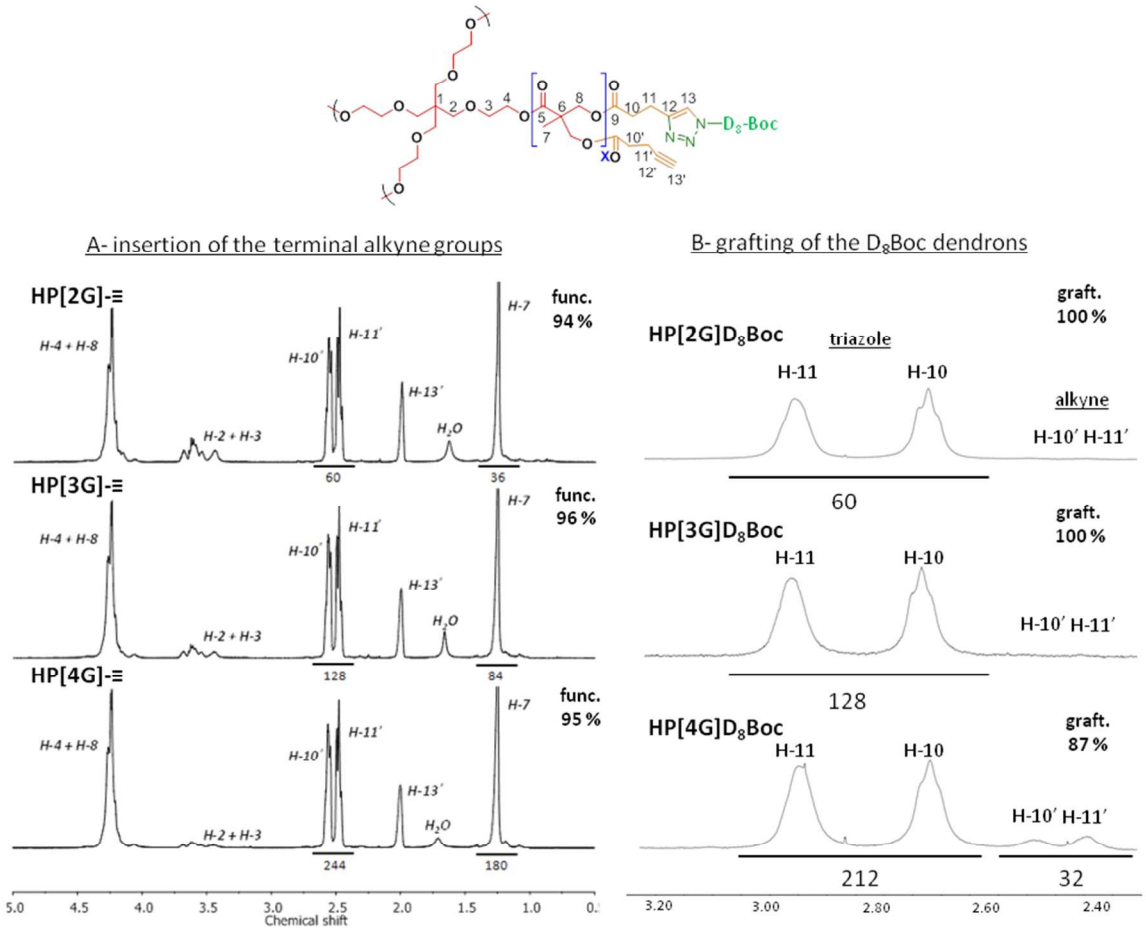

Figure 1. A. ^{1}H NMR spectra of **HP[2G]-≡**, **HP[3G]-≡** and **HP[4G]-≡** from 0 to 5 ppm in $CDCl_3$. The degree of functionalization was calculated from the relative integration of the signal for H-7 in comparison with those of H-10' and H-11'. **B.** ^{1}H NMR spectra of **HP[2G]D$_8$Boc**, **HP[3G]D$_8$Boc** and **HP[4G]D$_8$Boc** from 2.30 to 3.30 ppm in $CDCl_3$. The degree of grafting was calculated from the relative integrations of signals H-10 and H-11 (near to the triazole ring) in comparison with those of the H-10' and H-11' (near to the free alkyne groups).

The same two methylene protons (H-10' and H-11') were used to determine the number of D_8Boc dendrons that were grafted during the CuAAC reaction. When the triazole was formed these peaks moved to lower field, i.e., from 2.55 and 2.44 to 2.74 and 2.97 ppm, respectively (Figure 1B). In the case of HP[2G]D_8Boc and HP[3G]D_8Boc, peaks corresponding to the protons in the α- (H-11') and in β-positions (H-10') of the alkyne groups were not observed; indicating that complete functionalization of the peripheral alkyne groups had been achieved. Accordingly, 15 and 31 dendrons had been incorporated into HP[2G] and HP[3G], respectively. In contrast, two small peaks corresponding to the protons H-10' and H-11' were observed in the ^{1}H NMR spectrum of HP[4G]D_8Boc. This indicates that not all of the peripheral alkyne groups had reacted with a dendron. From the corresponding peak integrations it was estimated that around 53 dendrons could be grafted onto HP[4G], leaving an average of 8 non-functionalized terminal alkyne groups.

According to these data, the pseudodendrimers HP[2G]D_8Boc, HP[3G]D_8Boc and HP[4G]D_8Boc bear 120, 248 and 424 peripheral amino groups, respectively.

Further evidence for the formation of the pseudodendrimers was provided by the FTIR spectra (see SI-4). Firstly, after the addition of the terminal alkynes the band due to O−H st (3420 cm^{-1}) completely disappeared and two new bands, assigned to the ≡C−H st (3287 cm^{-1}) and C≡C st (2122 cm^{-1}) were observed. After the CuAAC reaction, the bands corresponding to the azide group of the free dendron (2102 cm^{-1}) and the alkyne groups of the hyperbranched polymers (3287 and 2122 cm^{-1}) were no longer observed.

Finally, SEC data (see SI-5) showed that retention times decreased after the insertion of peripheral alkyne groups on the commercial hyperbranched polyester and, more significantly, after the insertion of the D_8Boc dendrons due to the formation of the pseudodendrimers. Peaks

corresponding to the D_8Boc free dendron or other residues were not observed. The polydispersity of the final pseudodendrimers was quite low, with values between 1.13 and 1.22.

Finally, deprotection of the amino groups was evaluated by the disappearance of the signals corresponding to the *tert*-butoxycarbamate (*t*-Boc) groups in the NMR (see SI-3, Figure SI-3-2) and FTIR (see SI-4) spectra. In addition, in the FTIR spectra the N–H st band increased in intensity and this confirmed protonation of the terminal amino groups.

This original synthesis of *bis*-MPA pseudodendrimers by combining hyperbranched polymers and dendrons through click-chemistry reactions allowed us to obtain high-generation dendritic macromolecules with good global yields (21–25%) with respect to the synthesis of dendrimers. The polydispersity of the derivatives was rather low while the synthetic effort remained reasonable as only 11 steps are required.

3.2. Synthesis and characterization of the pseudodendrimers with a fluorescent marker HP[2G]D_8-(RhB) and HP[3G]D_8-(RhB). In order to observe the internalization of the pseudodendrimers and ascertain where the dendriplexes are located inside the cells, two of the three pseudodendrimers were covalently marked with rhodamine B, RhB, as a fluorophore.

The synthesis of these two pseudodendrimers, HP[2G]D_8-(RhB) and HP[3G]D_8-(RhB), was carried out in three steps by the CuAAC reaction (see SI). Firstly, the hyperbranched polyester cores with peripheral alkyne groups, HP[2G]-≡ and HP[3G]-≡, were functionalized with D_8Boc dendrons using a lower ratio D_8Boc/HP[2,3G]-≡ than that employed for complete functionalization. Secondly, the remaining free alkyne groups were reacted with an azide-rhodamine B derivative. The pseudodendrimers marked with rhodamine B, HP[2G]D_8Boc-(RhB) and HP[3G]D_8Boc-(RhB), were obtained in yields of 53 and 50%, respectively, which were slightly lower than those achieved with the pseudodendrimers without the rhodamine B marker.

Unfortunately, HP[4G]D_8Boc-(RhB) could not be obtained due to difficulties encountered in the purification process.

As described above, the success of the two CuAAC reactions was confirmed by FTIR and NMR. In the FTIR spectra the disappearance of the band corresponding to the azide group (2102 cm^{-1}) was observed. In the ^{1}H NMR spectra a peak corresponding to the triazole proton (H-13) was observed at 7.35 ppm along with the four –CH_2– protons in the α- and β-positions of the triazole ring in the hyperbranched polyester part (H-10 and H-11 protons). Signals for the protons in the dendritic part (H-14 and H-15 protons) were shifted to lower field (for proton numbering see Scheme SI-6). The insertion of the rhodamine B fluorophore was confirmed by the appearance of new peaks in the aromatic region of the spectra and by the presence of a peak at 3.63 ppm, which corresponds to the –N–(C$\underline{H_2}$–CH_3)$_2$ (H-25 in Scheme SI-6) of the rhodamine moiety.

The integration of the peaks corresponding to the methylene protons in the α- and β-positions of the triazole ring (H-11 and H-10, respectively) was again used to evaluate the degree of both D_8Boc dendron and rhodamine B grafting (Figure SI-6). Examination of the ^{1}H NMR spectra of the products obtained after grafting with D_8Boc dendrons and grafting with RhB indicated that approximately 13 D_8Boc dendrons and 1 molecule of rhodamine B had been incorporated into the 2nd generation hyperbranched polyester core, HP[2G]D_8Boc-(RhB), and 24 D_8Boc dendrons and 7 molecules of rhodamine B had been incorporated into the 3rd generation hyperbranched polyester core.

Finally, complete removal of the *t*-Boc protecting groups was confirmed, as described above, by FTIR and ^{1}H NMR by the disappearance of the signals corresponding to the carbamate group.

3.3. Dendriplex formation, dendriplex sizes, morphologies and ζ potential, dendriplex stability. To achieve efficient gene delivery a gene carrier must be able to bind pDNA into compact and positively charged complexes. The ability of the pseudodendrimers to efficiently complex and condense the plasmid DNA was studied at room temperature by gel retardation, EtBr displacement and ζ potential, while the dendriplexes were characterized by DLS and cryoTEM. The stability of the dendriplexes was also studied by gel retardation at 37 ºC.

Agarose gel retardation assay

The gel electrophoresis results indicate that all three pseudodendrimers showed good complexation to pDNA, even at low pseudodendrimer:pDNA w:w ratios, which started at 3:1 for HP[3G]D_8 and HP[4G]D_8 and 5:1 for HP[2G]D_8 (Figure 2a).

In order to compare our dendritic macromolecules with commercial reagents, Lipofectamine 2000 (a liposomal-based formulation) and TransIT-X2 (a polymer-based formulation) were used at the ratios recommended by the manufacturer. There is only a marginal difference in pDNA-retardation ability, starting with Lipofectamine at 3:1 (w:w) and TransIT-X2 at 2:1 (v:w), followed by HP[3G]D_8 and HP[4G]D_8 and finally HP[2G]D_8. Even though the number of peripheral amine groups is an important feature that determines the capacity of the dendritic material to complex pDNA, these results suggest that there is no significant difference between HP[2G]D_8, HP[3G]D_8 and HP[4G]D_8 despite the different numbers of terminal amine groups (120, 248 and 424, respectively). In terms of the number of charged nitrogen atoms (N^+) per μg of pseudodendrimer, all three dendritic derivatives show similar nmol(N^+)/μg values, and this could explain the similarities found in the complexation determined as a w:w ratio. Complexation ratios correspond to N/P = 7 for HP[2G]D_8 and N/P = 4 for HP[3G]D_8 and HP[4G]D_8, and these values are comparable to the N/P ratios obtained with similar dendritic

materials based on *bis*-MPA.[25] Thus, the difference between the materials resides in the number of molecules of each pseudodendrimer that is needed for complex formation, being 544 for HP[2G]D_8, 158 for HP[3G]D_8 and 91 for HP[4G]D_8 (see Table SI-7).

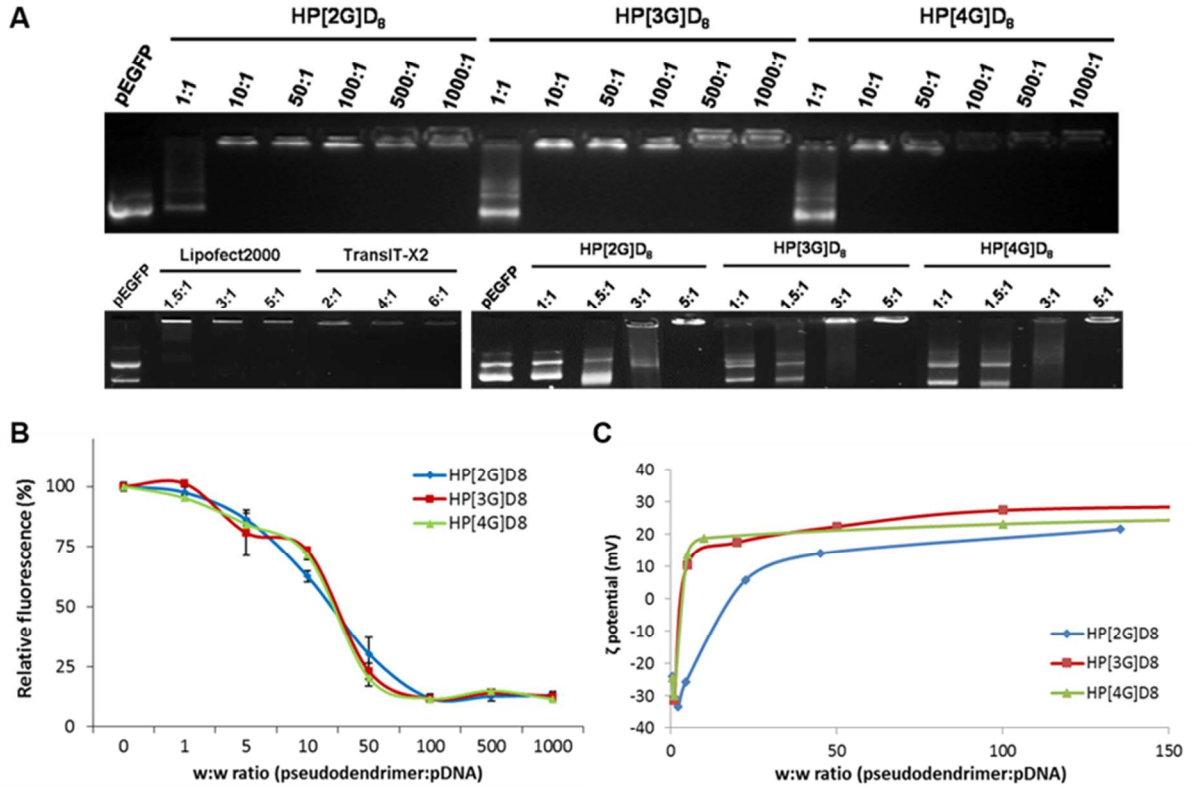

Figure 2. Complex formation and condensation. **A**. Electrophoretic mobility of free and complexed pDNA in SFM. Gel retardation of pDNA in the presence of increasing concentrations of the pseudodendrimers (w:w) (above) and comparison of the complexation ability of commercial reagents at recommended concentrations of (w:w) for lipofectamine and (v:w) for TransIT-X2 (below left) and pseudodendrimers (w:w) (below right). **B.** EtBr displacement by the three pseudodendrimers. Data are represented as a gradual decrease in % Fluorescence Intensity of EtBr for ratios of 1:1 to 1000:1 (w:w). Data are normalized to the fluorescence intensity of free pDNA. HP[2G]D_8 in blue, HP[3G]D_8 in red and HP[4G]D_8 in green. **C.** pDNA titration studied by ζ potential for the three pseudodendrimers; HP[2G]D_8 in blue, HP[3G]D_8 in red and HP[4G]D_8 in green.

Ethidium bromide competition assay. The binding capacities of the three complexes were further investigated by the EtBr exclusion assay. The EtBr dye intercalates with free pDNA and this results in a significant increase in fluorescence intensity. When the pseudodendrimers complex the pDNA, thus replacing the EtBr, the fluorescence intensity decreases (Figure 2b). The three pseudodendrimers have a similar efficiency and the same trend was observed in all cases. The fluorescence gently decreases at ratios of less than 10:1. A sharp decrease is observed with a displacement of 80% of the dye between the ratios 10:1 and 50:1. This demonstrates the cooperative binding of the dendrimers with the pDNA. However, and even if the pseudodendrimers can complex the pDNA at low ratios, as previously observed in the gel retardation assay (Figure 2a) these compounds cannot replace a high quantity of dye. Only loosely formed dendriplexes must be present at low pseudodendrimer:pDNA ratios and under these conditions the pseudodendrimer is unable to replace all of the intercalated dye. Ratios higher than 50:1 are required to replace high quantities of EtBr to afford more compact dendriplexes.

ζ potential. The ζ potential of the dendriplexes at different pseudodendrimer:pDNA ratios was measured (Figure 2c and Table 1). In all cases, the charge changes from negative values at low pseudodendrimer:pDNA ratios to positive values at high ratios. At ratios greater than 50:1, when the pDNA is totally complexed by the pseudodendrimers, the three dendriplexes interestingly exhibit a positive net charge of around +20 mV. The positive charge favors the interactions with glycoproteins, proteoglycans and glycerol phosphates, which are negatively charged molecules that belong to the cell membranes. An increase in the positive surface charge of the complexes might promote their uptake but it may also increase their cytotoxicity due to membrane destabilization. As a consequence, an appropriate balance between cellular uptake rate and

cytotoxicity is required to achieve optimal delivery and transgene expression. Additionally, complete complexation of the pDNA by the pseudodendrimers can be observed by this technique. This situation corresponds to the ratio at which a change occurs in the slope of the curve. According to these measurements, all of the pseudodendrimers can complex pDNA but HP[3G]D_8 and HP[4G]D_8 appear to be better than HP[2G]D_8.

Sizes and morphologies. The size and the morphology of the dendriplexes were determined by dynamic light scattering (DLS) and cryogenic transmission electron microscopy (cryoTEM) at two w:w ratios – 10:1 and 100:1 (Table 1 and Figure 3). Good agreement was observed for the results obtained by the two techniques. All of the dendriplexes have a spherical shape. HP[3G]D_8 and HP[4G]D_8 can form positively charged dendriplexes with a size of around 100 nm whereas HP[2G]D_8 only forms positively charged dendriplexes at the 100:1 ratio. As a general trend, the average sizes of the dendriplexes decrease on increasing the generation of the corresponding hyperbranched polymeric core. Thus, HP[2G]D_8 formed the biggest dendriplexes whereas HP[4G]D_8 formed the smallest ones. These sizes are appropriate for good cellular uptake mediated by endocytosis.[49-50]

Comparison of the data obtained for the two different generation ratios, i.e., 10:1 and 100:1, shows that the average sizes of the dendriplexes tend to decrease and their positive charge tends to increase on increasing the proportion of pseudodendrimers, thus providing more compact and positively charged dendriplexes. As observed in the EtBr exclusion assay (Figure 2c), even when the pseudodendrimers can form dendriplexes at ratios of less than 10:1, compact and positively charged dendriplexes that would better protect and transport the pDNA are only formed at ratios above 50:1.

Table 1. Size in nm and ζ potential of the pseudodendrimers and the dendriplexes at the w:w ratios 1:10 and 1:100 as measured by cryoTEM and TEM or DLS.

	dendriplexes w:w 10:1			dendriplexes w:w 100:1		
	DLS	cryoTEM	ζ pot.	DLS	cryoTEM	ζ pot.
$HP[2G]D_8$	122 +/- 47	157 +/- 31	- 15	88 +/- 20	128 +/- 24	+ 19
$HP[3G]D_8$	95 +/- 37	73 +/- 16	+ 20	112 +/- 38	103 +/- 37	+ 27
$HP[4G]D_8$	75 +/- 38	70 +/- 18	+ 19	64 +/- 31	54 +/- 20	+ 23

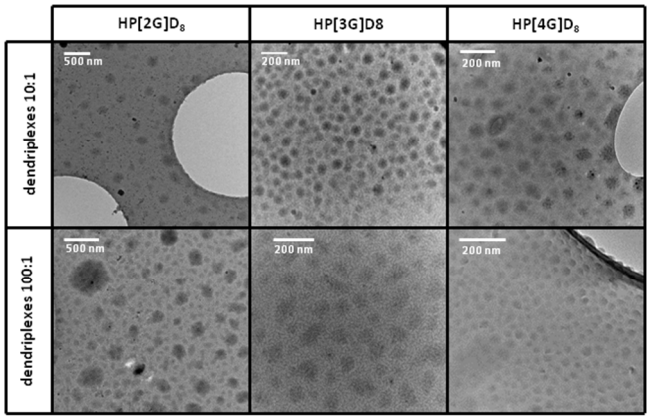

Figure 3. CryoTEM images of the dendriplexes at w:w ratios 10:1 and 100:1.

Dendriplex stability. The stability of the dendriplexes was studied by gel retardation assays under different conditions. Incubation of the corresponding pseudodendrimer and pDNA was carried out at room temperature in three different media, H_2O, SFM or DMEMc, and dendriplexes were then maintained at room temperature or 37 ºC for different times. At room temperature differences were not observed in complex stability for dendriplexes formed in H_2O, SFM or DMEMc (Figure SI-7a).

As can be observed for HP[2G]D_8, after incubation of the dendriplexes at 37 ºC in SFM for up to 1.5 hours, pDNA was gradually released over time (Figure 4a). After incubation for 4 hours in both culture media, pDNA was released from dendriplexes up to a ratio of 100:1 (w:w), although for HP[3G]D_8 and HP[4G]D_8 some retention was observed at this ratio (Figure 4b and Figure SI-7b).

In summary, all three pseudodendrimers can complex pDNA to form dendriplexes. HP[3G]D_8 and HP[4G]D_8 show a similar trend whereas HP[2G]D_8 appears to be less efficient. Although the dendriplexes can be formed starting at pseudodendrimer:pDNA ratios of less than 10:1 (see section 3.4.1), positively charged and compact dendriplexes that are sufficiently stable for gene delivery are formed at ratios higher than 50:1.

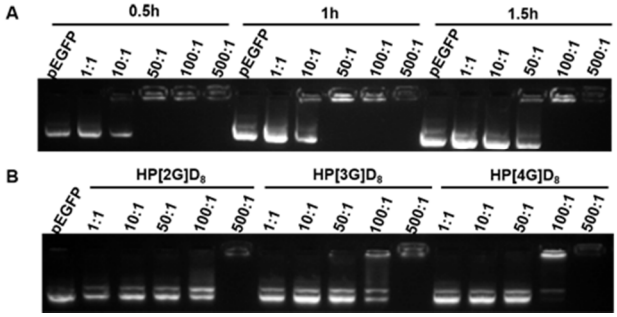

Figure 4. Stability of the dendriplexs in SFM. **A.** Gel retardation after incubation of the dendriplexes formed with HP[2G]D_8 at 37 ºC for 0.5 h, 1 h and 1.5 h. **B.** Gel retardation of the dendriplexes formed between the three pseudodendrimers and pDNA after incubation at 37 ºC for 4 h.

3.4. Cell viability. Other important requirements for a good gene carrier are low toxicity, as this can be a major limitation for the use of new cationic dendrimers for gene delivery, and biodegradability, in order to avoid the accumulation of the gene or drug carriers inside tissue. [51, 52] The three pseudodendrimers were found to be non-toxic at doses from 0.1 mg/mL to 1 mg/mL between 24 hours and 72 hours, with cell viability values above 80% for MSCs and HeLa

(Figure 5 and Figure SI-8-1). The absence of cytotoxicity was further confirmed by cell cycle analysis, where the percentage of cells in each phase remained constant. The pseudodendrimer size or the number of amine groups did not have any influence on the level of toxicity. These pseudodendrimers are based on bis-MPA hyperbranched polymers and dendrons; the degradability in aqueous solution of similar derivatives has already been demonstrated.[29, 41] Neither the pseudodendrimers nor the by-products that may accumulate during the degradation process (see SI-9) affect cell viability, meaning that the pseudodendrimers could be used in subsequent transfection experiments.

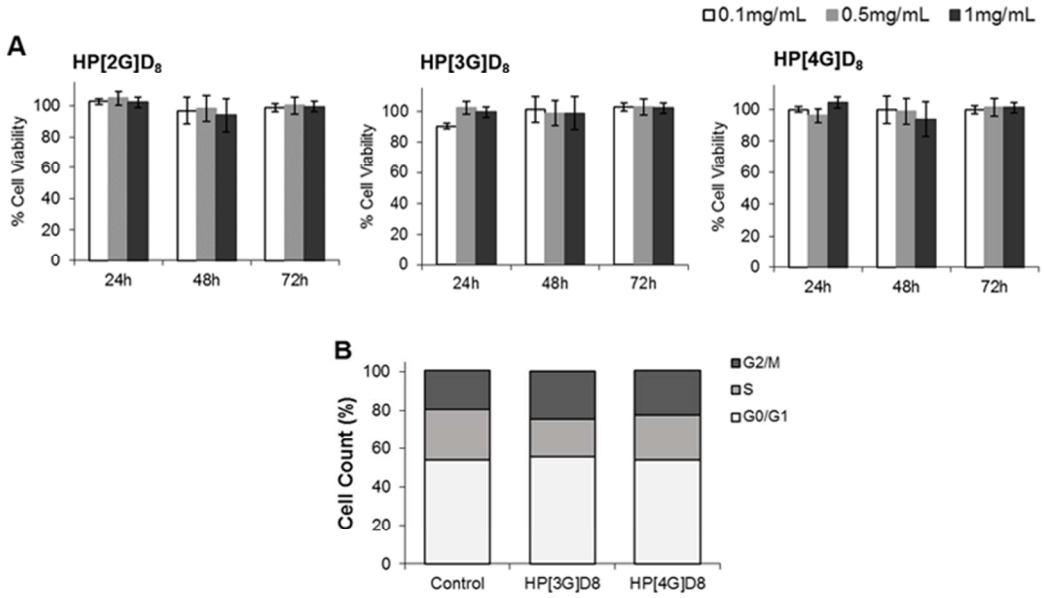

Figure 5. Toxicity of the three pseudodendrimers on MSCs in DMEMc. **A.** Cell Viability was analyzed by the Alamar Blue® assay and the fluorescence was normalized to cells receiving medium alone. **B.** Effect of 1 mg/mL of $HP[3G]D_8$ and $HP[4G]D_8$ exposure for 24 h on the phases of the cell cycle.

3.5. Transfection. Based on the results of the physico-chemical characterization of dendriplexes in terms of the size distribution, zeta potential and complexation efficiency, none of the pseudodendrimers could be ruled out as candidates for transfection, even if higher generation

dendrimers seem to be more promising due to their higher stability. To evaluate the transfection efficiency, dendriplexes at different ratios and under different conditions were incubated with HeLa and MSCs for 4 hours or 24 hours. The samples were removed and the cells were allowed to grow for up to 48 hours. EGFP relative fluorescence was then quantified on a fluorescence microscope, on a flow cytometer and on a microplate reader, and the cell viability was assessed by the Alamar Blue® assay (Figure 6).

HP[3G]D_8 and HP[4G]D_8 were able to transfect a small number of HeLa cells at ratios of 10:1 and 50:1 when complexes were first incubated for 30 minutes at 4 ºC and then maintained at 37 ºC (Figure SI-8-2). Nevertheless, on MSCs of mouse origin, the levels of transfection obtained with HP[4G]D_8 at 200:1 were similar to those obtained with commercial transfection agents such as Lipofectamine and TransIT-X2. At 100:1 the efficiency was half that obtained at 200:1 and a four-fold increase was achieved compared to HP[3G]D_8 at the same ratio. The GFP-positive populations obtained with the pseudodendrimers were similar to that obtained with TransIT-X2, and more homogenous than that obtained with Lipofectamine, with expression detected after 16 hours. GFP expression was not observed with HP[2G]D_8 at any ratio or HP[3G]D_8 and HP[4G]D_8 at low ratios. This lack of expression could be due to the dendriplexes being too large, poor condensation and prompt release of pDNA, which would not provide enough time for the dendriplexes to enter the cells or follow the correct endocytic pathway, thus resulting in pDNA degradation on the cytoplasm or lysosomes. The results demonstrate a dependence of transfection efficiency on the pseudodendrimer generation, w:w ratio and µg of pDNA. Although the results obtained with the three methods show a similar trend (higher efficiency with increasing generation and w:w ratio), the fluorescence microscopy and microplate reader techniques measure the total fluorescence intensity and cells that produce smaller amounts of

GFP are difficult to detect, whereas flow cytometry analyses cells individually, which could explain the higher percentage of GFP-positive cells detected on using Lipofectamine.

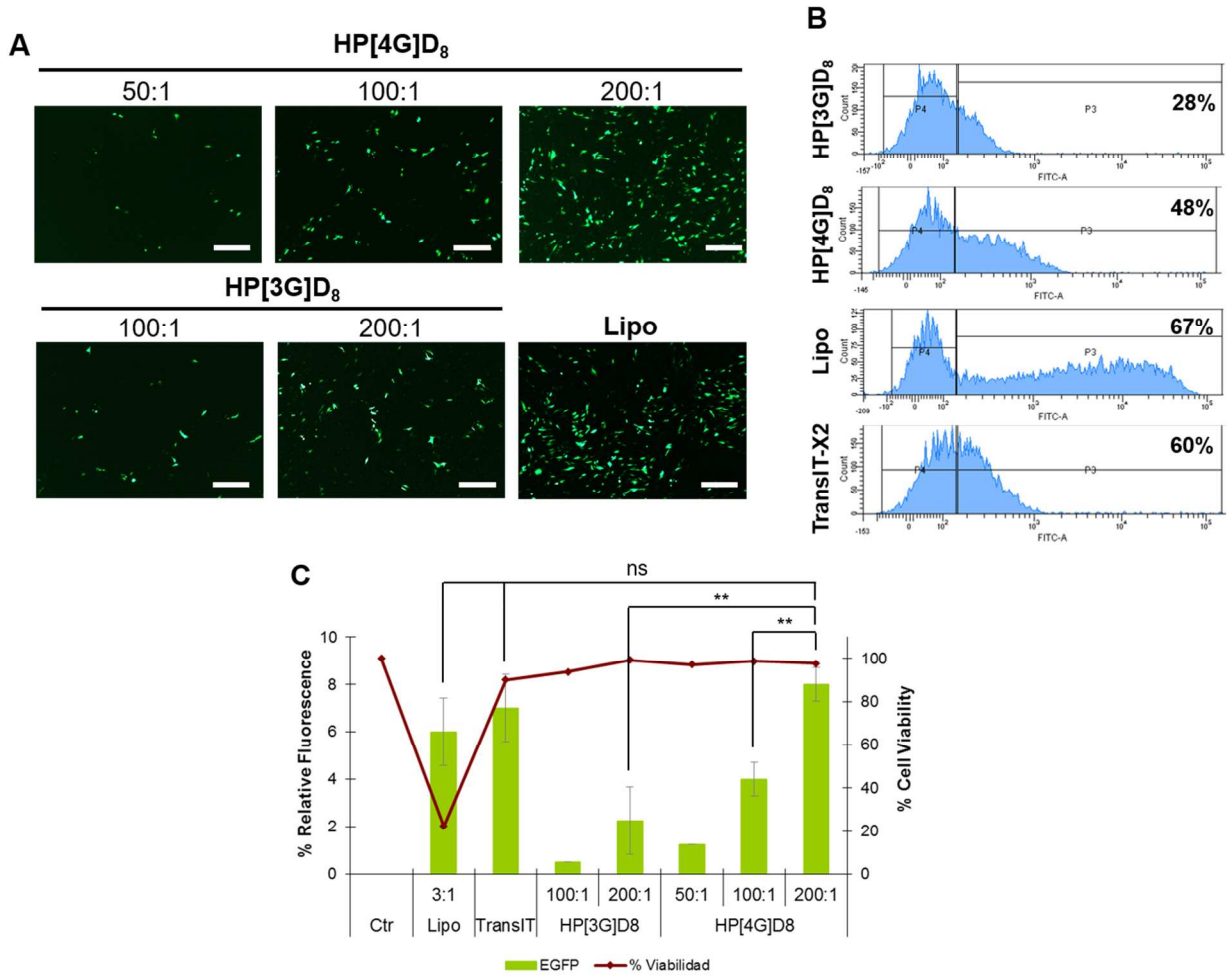

Figure 6. Transfection efficiency of HP[3G]D_8 and HP[4G]D_8 at different ratios (0.2 µg pEGFP) and Lipofectamine (0.1 µg pEGFP) and TransIT-X2 (0.1µg pEGFP) in SFM at 48 h on MSCs. **A.** Fluorescence images of cells expressing GFP after 4 h incubation. Scale bar = 100 µm. **B.** Flow cytometry histograms showing % of GFP-positive cells and fluorescence intensity after 4 h incubation. **C.** Relative intensity of GFP expression and cell viability after incubation of dendriplexes for 24 h (** $p<0.01$, ns $p>0.05$).

It should be emphasized that dendriplexes showed high cell viability even after incubation for 24 hours, and this is in contrast to commercial Lipofectamine, which was cytotoxic (Figure 6C and SI-8-1).

3.6. Uptake & intracellular distribution of the dendriplexes. Studies on the cellular uptake were carried out to evaluate the transfection efficiency. Firstly, HP[3G]D_8-RhB alone was incubated for different times (Figure 7).

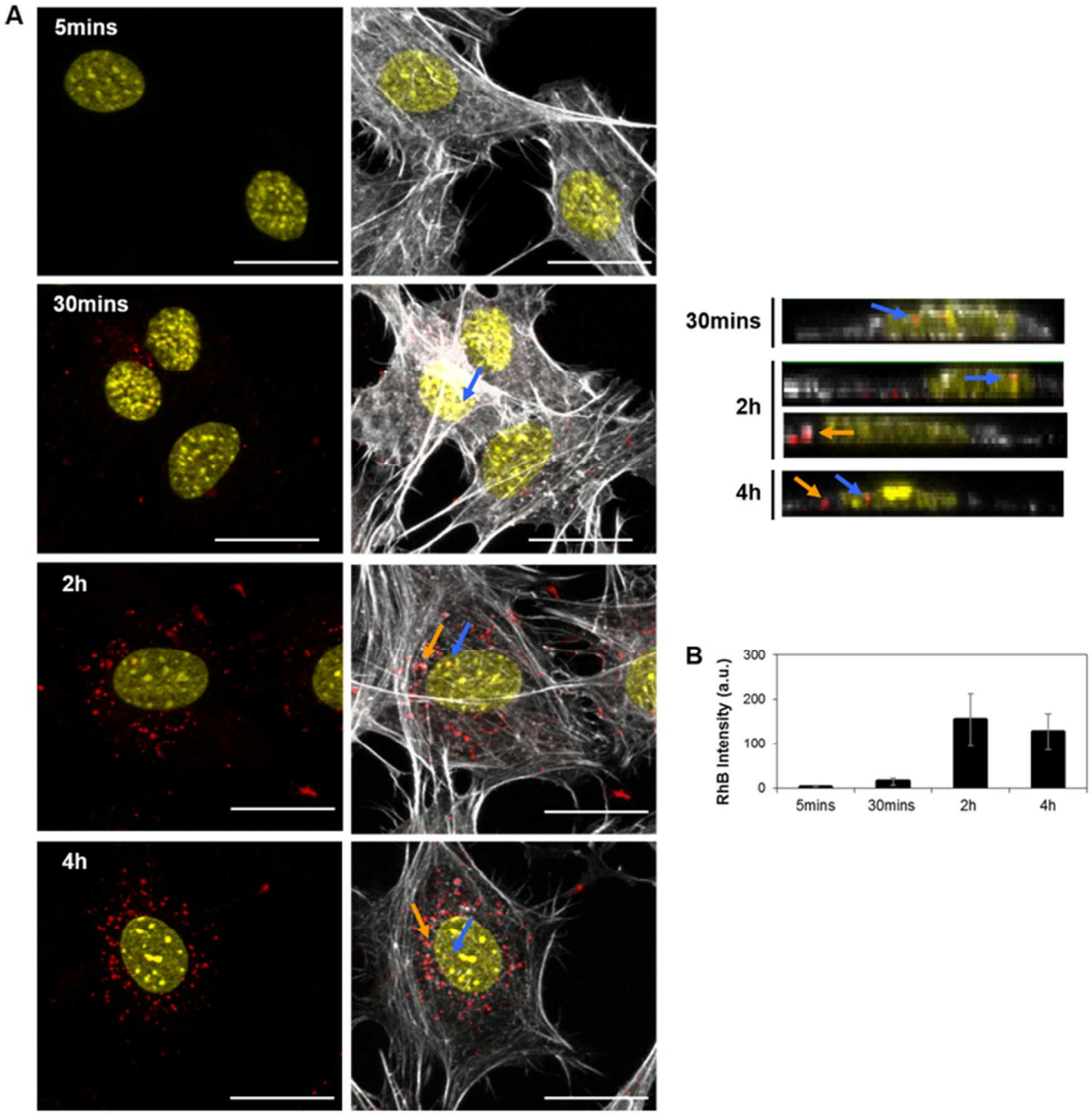

Figure 7. HP[3G]D_8-RhB internalization in MSCs. **A.** Confocal z-stack projections and corresponding lateral views. Arrows indicate colocalization of HP[3G]D_8-RhB with nuclei (blue) or actin (orange). Nuclei were stained with DAPI (yellow), actin filaments with AlexaFluor 488-Phalloidin (gray) and HP[3G]$D_8$with RhB (red). Scale bars: 20 μm. **B.** Relative quantification of confocal images of the internalized HP[3G]D_8-RhB.

Representative confocal images show the distribution of the pseudodendrimers along the cytoplasm and the higher colocalization with actin at 30 minutes and 2 hours, with higher accumulation around the nucleus with increasing time. However, HP[3G]D_8-RhB was found to colocalize with the nucleus after only 30 minutes. The difference in relative mean intensity of RhB from the confocal images could be due to the greater deviation between the internalization of each cell at 2 hours.

The internalization of dendriplexes formed between HP[4G]D_8 and Cy5-labeled pEGFP was analyzed at different times and compared to HP[3G]D_8 and Lipofectamine (Figure 8 and SI-10-1). Confocal microscopy showed efficient membrane binding at 30 minutes and internalized dendriplexes appear as dot-like structures, which is indicative of vesicle entrapment, with a gradual accumulation inside cells and progression towards the nucleus over time. Larger aggregates are seen at 4 hours and these are related to endosome fusion and to gradual dissociation of pEGFP. Colocalization with actin increased after 30 minutes and this was maintained between 2–4 hours. At 24 hours disseminated fluorescence and punctuated structures were present. This observation reflects the presence of dendriplexes captured in endosomes and released pEGFP.

Although the size and distribution of the dendriplexes and lipoplexes and the relative mean fluorescence intensity measured from the confocal images show similar levels of Cy5 for HP[4G]D_8, HP[3G]D_8 and Lipofectamine, flow cytometry results after extensive washing with

PBS-Glycine at low pH show lower intensity for HP[4G]D_8 at 50:1, HP[3G]D_8 at 200:1 and Lipofectamine, meaning that a lower level of internalization is obtained (Figure SI-10-1). Reduced uptake in the presence of NaN_3, a metabolic inhibitor, indicates that nanoparticles are internalized by an active energy-dependent process. The significant suppression of internalization after incubation of cells with $NaClO_3$, a specific inhibitor of proteoglycan sulfation, confirmed that the negative charge present in the cell membrane is essential for effective dendriplex binding and internalization.

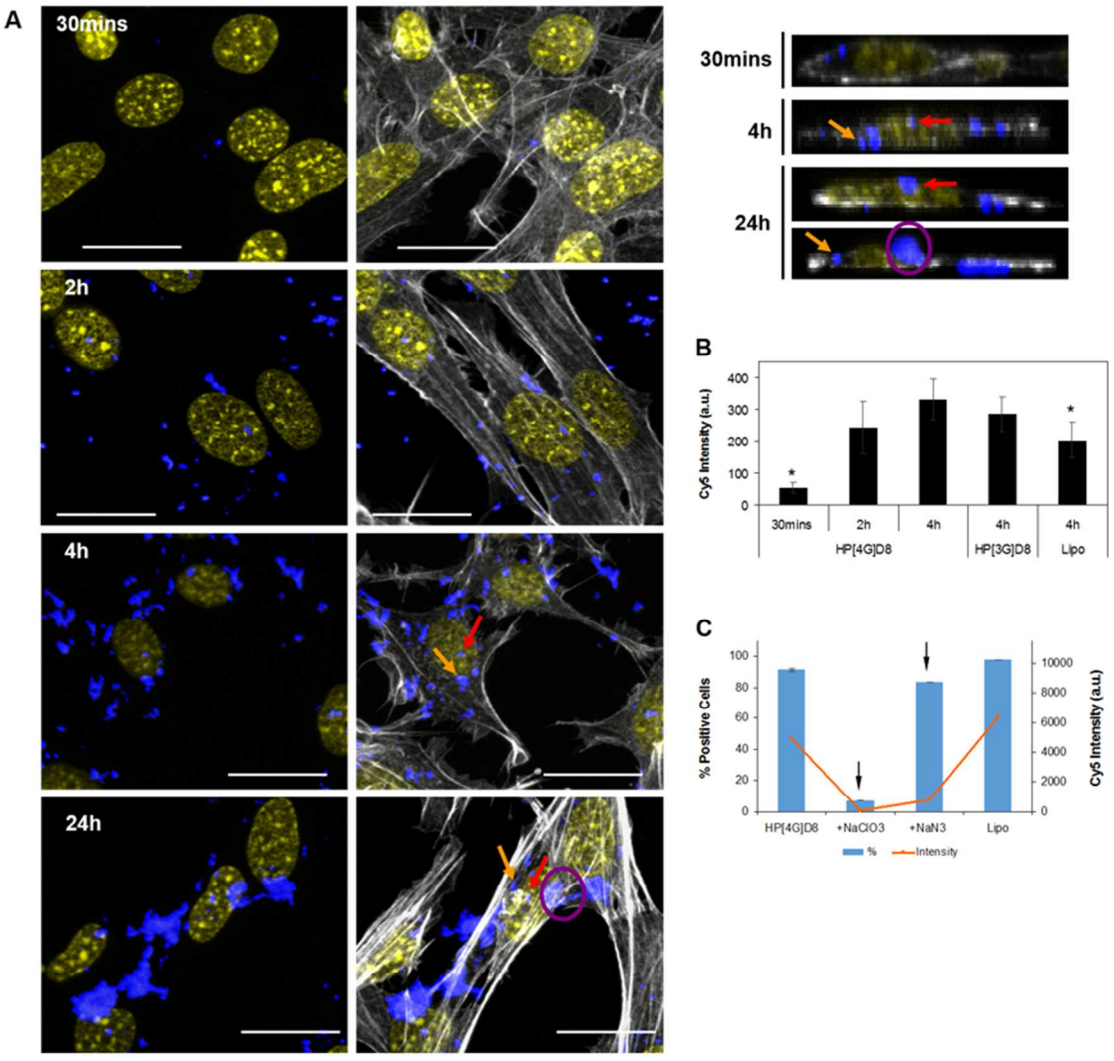

Figure 8. Internalization of dendriplexes of HP[4G]D_8@pEGFP-Cy5 in MSCs. **A.** Confocal z-stack projections and corresponding lateral views. Arrows indicate colocalization of dendriplexes with nuclei (blue) or actin (orange), and

the purple circle indicates diffuse fluorescence from released pEGFP-Cy5. Nuclei were labeled with DAPI (yellow), actin filaments with AlexaFluor 488-Phalloidin (gray) and pEGFP with Cy5 (blue). Scale bars: 20 μm. **B.** Relative quantification of confocal images (* indicates statistical significance compared to HP[4G]D_8 4 h, $p<0.05$). **C.** Quantification by flow cytometry at 4 h. The bars represent the percentage of internalization and the red line the intensity of the signal of the pEGP-Cy5.

It can be seen from Figure 9 that there is low colocalization of HP[4G]D_8@pEGFP-Cy5 in late endosomes after 1 hour incubation (Pearson's coefficient = 0.19). Furthermore, HP[3G]D_8-RhB@pEGFP-Cy5 dendriplexes can be seen after incubation for 30 minutes and 4 hours (in purple), with increasing accumulation of free HP[3G]D_8-RhB with time, and colocalization in the nucleus and cytoplasm. Less colocalization of red (HP[3G]D_8-RhB) and blue (pEGFP-Cy5) is seen at 4 hours as the pseudodendrimer is released from the dendriplexes.

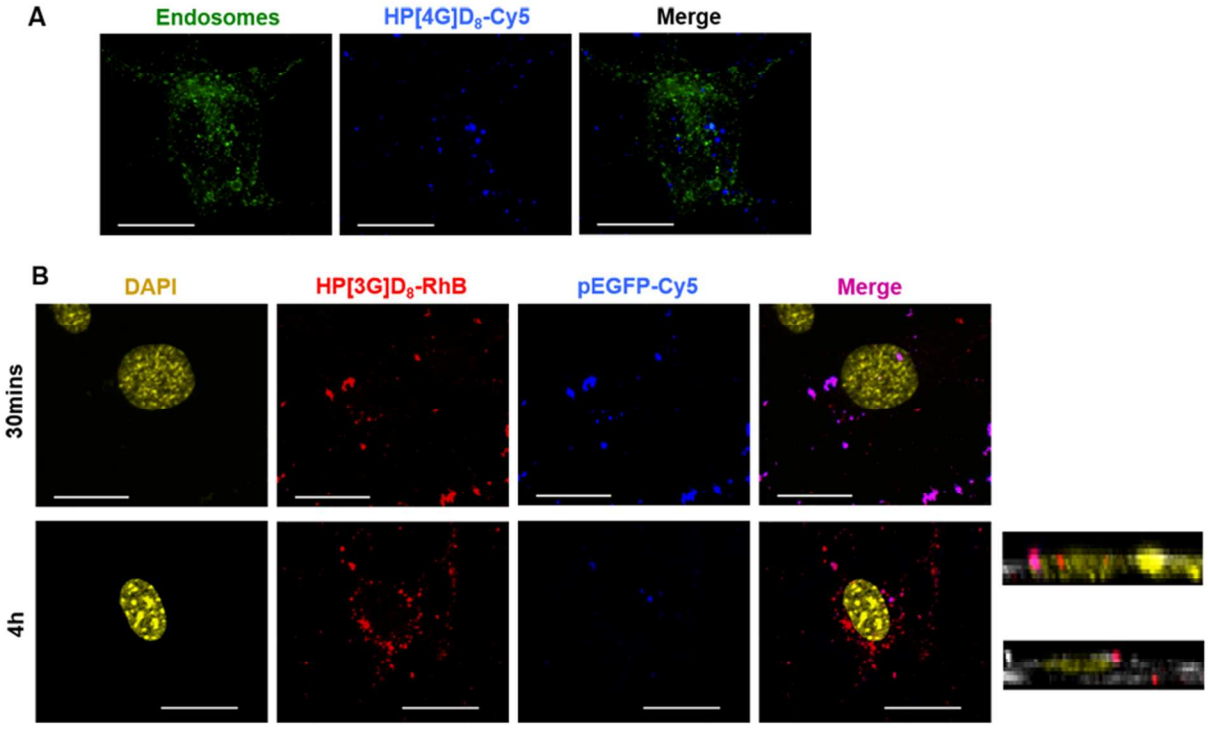

Figure 9. Internalization of dendriplexes in MSCs. **A.** Colocalization of HP[4G]D_8@pEGFP-Cy5 (blue) with early endosomes (GFP) after 1 h incubation. **B.** Confocal z-stack projections and corresponding lateral views with HP[3G]D_8-RhB@pEGFP-Cy5. Nuclei were labeled with DAPI (yellow), HP[3G]D_8 with RhB (red) and pEGFP with Cy5 (blue). Scale bars: 20 μm.

Since external primary amines have a pKa of around 9 and tertiary amines are not present, the primary amine groups will be protonated prior to endosome entry and they will not experience a marked change in protonation rate as the endosome acidifies, so a proton-sponge effect can be ruled out. However, the excess of pseudodendrimer could help to destabilize the membrane and generate imperfections that facilitate dendriplex release. Dendriplexes with larger sizes and surrounded by fewer free highly positive pseudodendrimers, as is the case for HP[2G]D8 or HP[3G]D8 and HP[4G]D8 at ratios below 200:1, may result in larger particles as pDNA decondensates that are either retained and degraded or exocytosed.[53-54]

As can be seen in Figure SI-10-2, HP[2G]D_8-RhB accumulates inside HeLa cells and quantification of RhB shows a fast initial internalization that is maintained with time, without diffusion of the pseudodendrimer at 4 ºC. Only a small number of dendriplexes can be found in the cytoplasm after 4–24 hours and the fluorescence intensity of Cy5 measured by flow cytometry has low values compared to those of commercial reagents. It is worth mentioning that the size of the complexes formed with the commercial reagent Lipofectamine is much larger than those formed with the derivatives described here (Figure SI-10-1). The size could be linked to plasmid condensation and release and, together with cellular membrane composition and endocytosis regulation, this could explain the inefficient transfection.

4. CONCLUSIONS

Three generations of new *bis*-MPA pseudodendrimers bearing 120, 248 and 424 terminal amino groups, respectively, have been successfully synthesized by copper(I) click chemistry. The compounds were totally biocompatible in the short and long term. The numerous terminal cationic moieties make all three generations efficient systems in terms of complex formation with pDNA and internalization inside mesenchymal stem cells. Efficient transfection on mesenchymal stem cells was dependent on generation. Higher generations were able to transfect these cells, without the need of further functionalization with specific ligands, at levels comparable to those shown by commercial reagents. To our knowledge, this is the first time that biocompatible and biodegradable dendritic *bis*-MPA-based macromolecules bearing primary terminal ammonium groups have been capable of transfecting MSCs at a level similar to the non-viral commercial transfection agents.

ASSOCIATED CONTENT

Supporting Information. Full synthesis and characterization data. Size exclusion chromatography of precursors. Complex formation and stability. Cytotoxicity and transfection on HeLa cells. Degradation studies. Internalization on MSCs and HeLa cells.

AUTHOR INFORMATION

Corresponding Author

*José Luis Serrano, joseluis@unizar.es. * Pilar Martín-Duque, mpmartind@gmail.com.

Author Contributions

The manuscript was written through contributions of all authors. All authors have given approval to the final version of the manuscript. * ‡ These authors contributed equally.

Funding Sources

ACKNOWLEDGMENTS

This work was financially supported by the MINECO-FEDER funds (under the projects CTQ2015-70174-P and MAT2015-66208-C3-1-P) and the Gobierno de Aragón-FSE (E04 research groups). A.L. thanks the MECD for his FPU grants (FPU12/05210) R.G. thanks DGA for his Phd grant. The authors would like the Laboratorio de Microscopia Avanzada, Instituto de Nanociencia de Aragon (LMA-Universidad de Zaragoza), Servicio General de Apoyo a la Investigación – SAI, Universidad de Zaragoza and Servicios Científico-Técnicos of CIBA (IACS) and CEQMA (UZ-CSIC) for access to instruments.

REFERENCES

(1) Naldini L. Gene therapy returns to centre stage. Nature **2015**, *526*, 351-360.

(2) Reiser J.; Zhang X.-Y.; Hemenway C. S.; Mondal D.; Pradhan L.; La Russa V. F.; Potential of mesenchymal stem cells in gene therapy approaches for inherited and acquired diseases. *Expert Opin. Biol. Ther.* **2005**, *5*,1571-1584.

(3) Dwyer R. M.; Khan S.; Barry F. P.; O'Brien T, Kerin M. J. Advances in mesenchymal stem cell-mediated gene therapy for cancer. *Stem Cell Res. Ther.* **2010**, *1*, 25-32.

(4) Crespo-Barreda A.; Encabo-Berzosa M. M.; González-Pastor R.; Ortiz-Teba P.; Iglesias M.; Serrano J. L.; Martin-Duque P. Viral and nonviral vectors for *in vivo* and *ex vivo* gene therapies. Laurence J.; Baptista P.; Naldini L. (Eds). Chapter 11 in Translating regenerative medicine to the clinic. Elsevier, 155-177.

(5) Bolhassani A.; Saleh T. Challenges in advancing the field of cancer gene therapy: an overview of the multi-functional nanocarriers. In Novel genes therapy approaches Wei M, Good D (Eds). Intech 2013.

(6) Prokop A.; Davidson J. M. Nanovehicular intracellular delivery systems. *J. Pharm. Sci.* **2008**, *97*, 3518-3590.

(7) Cotrim A. P.; Baum B. J. Gene therapy: some history, applications, problems, and prospects. *Toxicol. Pathol.* **2008**, *36*, 97-103.

(8) Mintzer M. A.; Simanek E. E. Nonviral vectors for gene delivery. *Chem. Rev.* **2009**, *109*, 259-302.

(9) Dizaj S. M.; Jafari S.; Khosroushahi A. Y. A sight on the current nanoparticle-based gene delivery vectors. *Nanoscale Res. Lett.* **2014**, *9*, 252-260.

(10) De Laporte L.; Cruz Rea J.; Shea L. D. Design of modular non-viral gene therapy vectors. *Biomaterials* **2006**, *27*, 947-954.

(11) Tomalia D. A.; Christensen, J. B.; Boas, U. *Dendrimers, Dendrons and Dendritic Polymers: Discovery, Applications and the Future*, Cambridge University Press, New York, 2012.

(12) Vögtle F.; Richardt G.; Werner N. *Dendrimer Chemistry, concepts, synthesis, porperties, applications*, Wiley-VCH Verlag GmbH & Co. KGaA, Weinheim, 2009.

(13) Kannan, R. M.; Nance, E.; Kannan, S.; Tomalia, D. A. Emerging concepts in dendrimer-based nanomedicine: from design principles to clinical applications, *J. Intern. Med.* **2014**, *276*, 579-617.

(14) Astruc D.; Boisselier E.; Ornelas C. Dendrimers designed for functions: from physical, photophysical and supramolecular properties to applications in sensing, catalysis, molecular electronics, photonics, and nanomedicine. *Chem. Rev.* **2010**, *110*, 1857-1959.

(15) Duncan R.; Izzo L. Dendrimer biocompatibility and toxicity. *Adv. Drug Deliv. Rev.* **2005**, *57*, 2215-2237.

(16) Haensler J.; Szoka F. C. Polyamidoamine cascade polymers mediate efficient transfection of cells in culture. *Bioconjugate Chem.* **1993**, *4*, 372-379.

(17) Zinselmeyer B.; Mackay S.; Schatzlein A.; Uchegbu I. The lower-generation polypropylenimine dendrimers are effective gene-transfer agents. *Pharm. Res.* **2002**, *19*, 960-967.

(18) Yamagata M.; Kawano T.; Shiba K.; Mori T.; Katayama Y.; Niidome T. Structural advantage of dendritic poly(l-lysine) for gene delivery into cells. *Bioorg. Med. Chem.* **2007**, *15*, 526-532.

(19) Jiménez J.; Clemente M.; Weber N.; Sánchez J.; Ortega P.; de la Mata F. J.; Gómez R.; García D.; López-Fernández L.; Muñoz-Fernández M. A.. Carbosilane dendrimers to transfect human astrocytes with small interfering RNA targeting human immunodeficiency virus. *BioDrugs* **2010**, *24*, 331-343.

(20) Merkel O. M.; Mintzer M. A.; Sitterberg J.; Bakowsky U.; Simanek E. E.; Kissel T. Triazine dendrimers as nonviral gene delivery systems: effects of molecular structure on biological activity. *Bioconjugate Chem.* **2009**, *20*, 1799-1806.

(21) Loup C.; Zanta M. A.; Caminade A. M.; Majoral J. P.; Meunier B. Preparation of water-soluble cationic phosphorus-containing dendrimers as DNA transfecting agents. *Chem. Eur. J.* **1999**, *5*, 3644-3650.

(22) Menuel S.; Fontanay S.; Clarot I.; Duval R. E.; Diez L.; Marsura A. Synthesis and complexation ability of a novel bis-(guanidinium)-tetrakis-(β-cyclodextrin) dendrimeric tetrapod as a potential gene delivery (DNA and siRNA) system. Study of Cellular siRNA transfection. *Bioconjugate Chem.* **2008**, *19*, 2357-2362.

(23) Liu X.; Zhou J.; Yu T.; Chen C.; Cheng Q.; Sengupta K. et al. Adaptive amphiphilic dendrimer-based nanoassemblies as robust and versatile siRNA delivery systems. *Angew. Chem. Int. Ed.* **2014**, *126*, 12016-12021.

(24) Liu H.; Wang H.; Yang W.; Cheng Y. Disulfide cross-linked low generation dendrimers with high gene transfection efficacy, low cytotoxicity, and low cost. *J. Am. Chem Soc.* **2012**, *134*, 17680-17687.

(25) Carlmark A.; Malmstrom E.; Malkoch M. Dendritic architectures based on bis-MPA: functional polymeric scaffolds for application-driven research. *Chem. Sci. Rev.* **2013**, *42*, 5858-5879.

(26) Van der Pol D. G.; Kieler-Ferguson H. M.; Floyd W. C.; Guillaudeu S. J.; Jerger K.; Szoka F. C.; Frechet J. M. Design, synthesis, and biological evaluation of a robust, biodegradable dendrimer. *Bioconjugate Chem.* **2010**, *21*, 764-773 and references therein.

(27) Twibanire J. A.; Grindley T. B. Polyester dendrimers: smart carriers for drug delivery. *Polymers* **2014**, *6*, 179-213.

(28) Feliu N.; Walter M. V.; Montañez M. I.; Kunzmann A.; Hult A.; Nyström A.; Malkoch M.; Fadeel B. Stability and biocompatibility of a library of polyester dendrimers in comparison to polyamidoamine dendrimers. *Biomaterials* **2012**, *33*, 1970-1981.

(29) Reul R.; Nguyen J.; Kissel T. Amine-modified hyperbranched polyesters as non-toxic, biodegradable gene delivery systems. *Biomaterials* **2009**, *30*, 5815-5824.

(30) Reul R.; Nguyen J.; Biela A.; Marxer E.; Bakowsky U.; Klebeb G.; Kissel T. Biophysical and biological investigation of DNA nano-complexes with a non-toxic, biodegradable amine-modified hyperbranched polyester. *Int. J. Pharm.* **2012**, *436*, 97-105.

(31) Movellan J.; González-Pastor R.; Martín-Duque P.; Sierra T.; De La Fuente J. M.; Serrano J.L. New ionic bis-MPA and PAMAM dendrimers: a study of their biocompatibility and DNA-complexation. *Macromol. Biosci.* **2015**, *15*, 657-667.

(32) Schallon A.; Jérôme V.; Walther A.; Synatschke C. V.; Müller A. H. E.; Freitag R. Performance of three PDMAEMA-based polycation architectures as gene delivery agents in comparison to linear and branched PEI. *Reac. Func. Polym.* **2010**, *70*, 1-10.

(33) Zhang Z.; Yin L.; Xu Y.; Tong R.; Lu Y.; Ren J.; Cheng J. Facile functionalization of polyesters through thiol-yne chemistry for the design of degradable, cell-penetrating and gene delivery dual-functional agents. *Biomacromol.* **2012**, *13*, 3456-3462.

(34) Lim Y. B.; Kim C. H.; Kim K.; Kim S. W.; Park J. S. Development of a safe gene delivery system using biodegradable polymer, poly(α-(4-aminobutyl)-l-glycolic acid). *J. Am. Chem. Sci.* **2000**, *122*, 6524-6525.

(35) Zheng Y.; Li S.; Weng Z.; Gao C. Hyperbranched polymers: advances from synthesis to applications. *Chem. Soc. Rev.* **2015**, *44*, 4091-4130.

(36) Irfan M.; Seiler M. Encapsulation using hyperbranched polymers: from research and technologies to emerging applications. *Ind. Eng. Chem. Res.* **2010**, *49*, 1169-1196.

(37) Yang X.; Grailer J. J.; Pilla S.; Steeber D. A.; Gong S. Tumor-targeting, pH-responsive and stable unimolecular micelles as drug nanocarriers for targeted cancer therapy. *Bioconjugate Chem.* **2010**, *21*, 496-504.

(38) Lederer A.; Burchard W.; Hartmannm T.; Haataja J. S.; Houbenov N.; Janke A.; Friedel P.; Schweins R.; Lindner P. Dendronized hyperbranched macromolecules: soft matter with a novel type of segmental distribution. *Angew. Chem. Int. Ed.* **2015**, *54*, 12578-12583.

(39) Lederer A.; Hartmann T.; Komber H. Sphere-Like Fourth Generation Pseudo-Dendrimers with a Hyperbranched Core. *Macromol. Rapid Commun.* **2012**, *33*, 1740-1744.

(40) Calderón M.; Quadir M. A.; Sharma S. K.; Haag R. R. Dendritic polyglycerols for biomedical applications. *Adv. Mater.* **2010**, *22*, 190-218.

(41) Movellan J.; Urbán P.; Moles E.; De La Fuente J. M.; Sierra T.; Serrano J. L.; Fernàndez-Busquets X. Amphiphilic dendritic derivatives as nanocarriers for the targeted delivery of antimalarial drugs. Biomaterials **2014**, *35*, 7940-7950.

(42) Lomba M.; Oriol L.; Alcalá R.; Sánchez C.; Moros M.; Grazú V.; Serrano J. L.; De La Fuente J. M. *In situ* photopolymerization of biomaterials by thiol-yne click chemistry. *Macromol. Biosci.* **2011**, *11*, 1505-1514.

(43) Jiménez-Pardo I.; González-Pastor R.; Lancelot A.; Clavería-Gimeno R.; Velázquez-Campoy A.; Abián O.; Ros M. B.; Sierra T. Shell cross-linked polymeric micelles as camptothecin nanocarriers for anti-HCV therapy. *Macromol. Biosci.* **2015**, *15*, 1381–1391.

(44) Wooley K. L.; Hawker C. J.; Fréchet J. M. J. Hyperbranched macromolecules *via* a novel double stage convergent growth approach. *J. Am. Chem. Soc.* **1991**, *113*, 4252-4261.

(45) a) Huisgen R. Centenary Lecture - 1,3-Dipolar Cycloadditions. *Proc. Chem. Soc.* **1961**, 357-396; b) Kolb HC, Finn MG, Sharpless KB. Click chemistry: diverse chemical function from a few good reactions. *Angew. Chem. Int. Ed.* **2001**, *40*, 2004-2021; c) Franc G.; Kakkar A. K. "Click" methodologies: efficient, simple and greener routes to design dendrimers. *Chem. Soc. Rev.* **2010**, *39*, 1536-1544.

(46) Ihre H.; Hult A.; Söderling E. Synthesis, characterization and 1H NMR self-diffusion studies of dendritic aliphatic polyesters based on 2,2-bis(hydroxymethyl)propionic acid and 1.1.1-tris(hydroxyphenyl)ethane. *J. Am. Chem. Soc.* **1996**, *118*, 6388-95.

(47) Himo F.; Lovell T.; Hilgraf R.; Rostovtsev VV, Noodleman L, Sharpless KB, Fokin VV. Copper(I)-catalyzed synthesis of azoles. DFT study predicts unprecedented reactivity and intermediates. *J. Am. Chem. Soc.* **2004**, *127*, 210-216.

(48) Chan T. R.; Hilgraf R.; Sharpless K. B.; Fokin V. V. Polytriazoles as copper(I)-stabilizing ligands in catalysis. *Org. Lett.* 2004, 6, 2853-2855.

(49) de Garibay A. P. R. Endocytosis in gene therapy with non-viral vectors. *Wien Med Wochenschr.* **2016**, *166*, 227-235.

(50) Oh N.; Park J-H. Endocytosis and exocytosis of nanoparticles in mammalian cells. *Int. J. Nanomedicine* **2014**, *9*, 51-63.

(51) Owens III D. E.; Peppas N. A. Opsonization, biodistribution, and pharmacokinetics of polymeric nanoparticles. *Int. J. Pharm.* **2006**, *307*, 93-102.

(52) Alexis F.; Pridgen E.; Molnar L. K.; Farokhzad O. C. Factors Affecting the Clearance and Biodistribution of Polymeric Nanoparticles. *Mol. Pharmaceutics* **2008**, *5*, 505-515.

(53) Singh J.; Michel D.; Chitanda J. M.; Verrall R. E.; Badea I. Evaluation of cellular uptake and intracellular trafficking as determining factors of gene expression for amino acid-substituted gemini surfactant-based DNA nanoparticles. *J. Nanobiotechnology* **2010**, *10*, 1-14.

(54) Zhang J.; Liu D.; Zhang M.; Sun Y.; Zhang X.; Guan G.; Zhao X.; Qiao M.; Chen D.; Hu H. The cellular uptake mechanism, intracellular transportation, and exocytosis of polyamidoamine dendrimers in multidrug-resistant breast cancer cells. *Int J Nanomedicine* **2016**, *11*, 3677-3690.